

AURORACAP: EFFICIENT, PERFORMANT VIDEO DETAILED CAPTIONING AND A NEW BENCHMARK

Anonymous authors

Paper under double-blind review

ABSTRACT

Video detailed captioning is a key task which aims to generate comprehensive and coherent textual descriptions of video content, benefiting both video understanding and generation. In this paper, we propose AURORACAP, a video captioner based on a large multimodal model. We follow the simplest architecture design without additional parameters for temporal modeling. To address the overhead caused by lengthy video sequences, we implement the token merging strategy, reducing the number of input visual tokens. Surprisingly, we found that this strategy results in little performance loss. AURORACAP shows superior performance on various video and image captioning benchmarks, for example, obtaining a CIDEr of 88.9 on Flickr30k, beating GPT-4V (55.3) and Gemini-1.5 Pro (82.2). However, existing video caption benchmarks only include simple descriptions, consisting of a few dozen words, which limits research in this field. Therefore, we develop VDC, a video detailed captioning benchmark with over one thousand carefully annotated structured captions. In addition, we propose a new LLM-assisted metric VDC-SCORE for better evaluation, which adopts a divide-and-conquer strategy to transform long caption evaluation into multiple short question-answer pairs. With the help of human Elo ranking, our experiments show that this benchmark better correlates with human judgments of video detailed captioning quality.

1 INTRODUCTION

The task of video detailed captioning involves generating comprehensive and coherent textual descriptions of video content, capturing not only the primary actions and objects but also intricate details, contextual nuances, and temporal dynamics. It has emerged as a critical area of research in computer vision and natural language processing, with significant implications for the fields of robotics (Yang et al., 2023b; Du et al., 2024), ego-centric perception (Grauman et al., 2022; 2023), embodied agents (Zhao et al., 2023; 2024c;d; Deng et al., 2023; 2024; Zhao et al., 2024b), and video editing (Chai et al., 2023) and generation (Bar-Tal et al., 2024). The challenges of video detailed captioning compared to past problems include the limited detailed caption data for training and evaluation, and also the lack of a good evaluation metric.

Before the emergence of Large Language Models (LLMs), previous models could only generate very short and rough descriptions of videos (Wang et al., 2022; Xu et al., 2023; Yan et al., 2022; Yang et al., 2023a). Although these models have been trained on web-scale video-text datasets (*e.g.*, HowTo100M (Miech et al., 2019) and VideoCC3M (Nagrani et al., 2022)), their capabilities remain limited due to their smaller scale and the lack of world knowledge possessed by LLMs. Recently, researchers start to build more powerful large multimodal models (LMMs) upon pretrained LLMs (*e.g.*, LLaVA (Liu et al., 2024b), InstructBlip (Dai et al., 2024b), InternVL (Chen et al., 2023b)). These models typically use intermediate components (*e.g.*, Q-Former (Li et al., 2023a) or an MLP) to connect the pre-trained vision transformer (ViT) (Dosovitskiy et al., 2020) and the LLM. Expanding from image-based LMMs to video-based LMMs is a natural progression, as videos can be viewed as sequences of frames. While most LMMs start with loading the pre-trained weights from image models and are further fine-tuned with video-text data, we find that LLaVA-like models can be easily adapted to a video one without any additional parameters but only with high-quality video-text instruction data for fine-tuning.

Table 1: **Benchmark comparison** for video captioning task. Ave. Length indicates the average number of words per caption. Compared to the existing benchmarks, VDC has the longest captions.

Dataset	Theme	# Video	# Clip	# Caption	# Word	# Vocab.	Ave. Length
MSVD (Chen & Dolan, 2011)	Open	1,970	1,970	70,028	607,339	13,010	8.67
MSR-VTT (Xu et al., 2016)		7,180	10,000	200,000	1,856,523	29,316	9.28
ActivityNet (Krishna et al., 2017a)		20,000	100,000	100,000	1,340,000	15,564	13.40
S-MiT (Monfort et al., 2021)		515,912	515,912	515,912	5,618,064	50,570	10.89
M-VAD (Torabi et al., 2015)	Movie	92	48,986	55,905	519,933	18,269	9.30
MPII-MD (Rohrbach et al., 2013)		94	68,337	68,375	653,467	24,549	9.56
Youcook2 (Zhou et al., 2018)	Cooking	2,000	15,400	15,400	121,418	2,583	7.88
Charades (Sigurdsson et al., 2016)	Human	9,848	10,000	27,380	607,339	13,000	22.18
VATEX (Wang et al., 2019)		41,300	41,300	413,000	4994,768	44,103	12.09
VDC (ours)	Open	1,027	1,027	1,027	515,441	20,419	500.91

However, naive treatment of videos as a series of image frames can result in significant computational overhead and may cause a generalization of the length problem (Wang et al., 2024b). To address these concerns, more specifically, to reduce the number of visual tokens, Video-LLaMA (Li et al., 2023f) adapts the video Q-former, MovieChat (Song et al., 2023) uses a memory bank, LLaMA-VID (Li et al., 2023g) simply uses global pooling, and FastV (Chen et al., 2024b) drops visual tokens by attention rank within LLM layers. In this paper, we present AURORACAP, adapting a simple yet efficient method called Token Merging (Bolya et al., 2022), which is proved to be effective in image and video classification and editing tasks (Li et al., 2023e). To be specific, we gradually combine similar tokens in a transformer layer using a bipartite soft matching algorithm to reduce the number of visual tokens. Following this pattern, our experiments show that we can use only 10% to 20% visual tokens compared to the original tokens generated by ViT with a marginal performance drop in various benchmarks. With this technique, it is easier to support higher-resolution and longer video sequence inputs for training and inference.

We present results on several widely used benchmarks, but find that existing video understanding benchmarks are either question-answer-based (Song et al., 2023; Chen & Dolan, 2011; Caba Heilbron et al., 2015; Xu et al., 2016; Xiao et al., 2021; Fu et al., 2024; Wu et al., 2024), which cannot demonstrate detailed descriptive abilities, or they provide descriptions that are too short, with only a few words (Xu et al., 2016; Caba Heilbron et al., 2015) as shown in Table 1. Some large-scale datasets focus on specific domains such as ego-centric (Grauman et al., 2023) or contain low-quality videos and annotations (Bain et al., 2021). Therefore, we construct the VDC (Video Detailed Captions) benchmark, which contains over one thousand high-quality video-caption pairs spanning a wide range of categories, and the resulting captions encompass rich world knowledge, object attributes, camera movements, and crucially, detailed and precise temporal descriptions of events. We utilize GPT-4o as our recaption assistant with a hierarchical prompt design. To preserve as much information as possible from the videos and maintain temporal consistency, we implement a dense-frame extraction strategy. Using the dense frames as input, despite description of the whole video, we also generate high-quality captions from different aspects, including objective facts, backgrounds, camera angles and movements. Manual quality inspection is employed to ensure the quality of the video captions. While existing video-caption datasets (Chen et al., 2024d; Ju et al., 2024; Li et al., 2024b) offer structured captions, VDC is the first benchmark focused on detailed video captioning, providing significantly longer and more detailed captions than others as shown in the Table 1 and Section D.

We also introduce a novel evaluation metric specifically designed for detailed captioning task. Traditional metrics like METEOR (Banerjee & Lavie, 2005), CIDEr (Vedantam et al., 2015), and BLEU (Papineni et al., 2002), designed for machine translation or short captions, fail to evaluate detailed captions which contain rich semantic information. On the other side, an LLM-based evaluation metric is commonly used in visual question answering benchmarks (Maaz et al., 2023; Wu et al., 2024), especially for those generated by VLMs (Song et al., 2024; 2023). However, we observe that the LLM-based evaluation metric still struggles to differentiate the quality of detailed captions and tends to give lower scores. To address these challenges, we propose VDCSCORE, a novel captioning evaluation metric that leverages the reliability of large language models (LLMs) by evaluating short visual question-answer pairs. We first decompose the ground-truth caption into a set of concise question-answer pairs using the LLM, then generate corresponding responses from the

108 predicted caption. Finally, the LLM is used to assess the accuracy of each response to provide an
 109 overall score. In particular, our paper makes the following contributions:

- 110 • In Section 2, we illustrate how we can reduce the number of tokens used for image or video
 111 input before injecting into LLM with marginal performance drop. Using these insights, we pro-
 112 pose AURORACAP, a video understanding base model with improved captioning performance,
 113 which also demonstrates advanced performance on existing benchmarks.
- 114 • In Section 3, we present VDC, the first benchmark for detailed video captioning, featuring over
 115 one thousand videos with significantly longer and more detailed captions. We comprehensively
 116 evaluate proprietary and open-source models using our proposed VDCSCORE metric. We also
 117 conduct extensive ablation studies based on AURORACAP.

118 2 AURORACAP: A VIDEO DETAILED CAPTIONING BASELINE

119 2.1 ARCHITECTURE

120 **Large multimodal model.** To effectively leverage the capabilities of both the pre-trained LLM
 121 and visual model, which is typically CLIP (Radford et al., 2021) or DINO (Oquab et al., 2023),
 122 LLaVA adapt a simple multi-layer perceptron (MLP) as projection layer to connect each patch
 123 tokens of image features into the word embedding space. The original LLaVA model is trained
 124 by a two-stage instruction-tuning procedure, which first pretraining projection layer for feature
 125 alignment and then finetuning end-to-end while freeze the visual encoder. Recent works like Prismatic
 126 VLMs (Karamcheti et al., 2024) and Idefics2 (Laurençon et al., 2024) further explore the design
 127 space of LLaVA architecture. We adapt some conclusion from those works for training the model.

128 **Token merging.** To increase the throughput of existing ViT models, Token Merging (Bolya et al.,
 129 2022) is proposed to gradually combines similar tokens in a transformer to reduce the number of
 130 tokens passing through ViT models. Token Merging has been proven to be effective on image and
 131 video classification tasks even without the need for training. Token Merging is applied between the
 132 attention and MLP within each transformer block as:

- 133 1. Alternatively partition the tokens into two sets \mathbb{A} and \mathbb{B} of roughly equal size.
- 134 2. For each token in set \mathbb{A} , calculate the token similarity with each token in set \mathbb{B} based on cosine
 135 similarity of the *Key* features in attention block.
- 136 3. Use bipartite soft matching and then select the most similar r pairs.
- 137 4. Merge the tokens using weighted average, record the token size.
- 138 5. Concatenate the two sets \mathbb{A} and \mathbb{B} back together again.

139 Once the tokens have been merged, they actually carry the features for more than one input patch.
 140 Therefore, the merged tokens will have less effect in softmax attention as

$$141 \mathbf{A} = \text{softmax} \left(\frac{\mathbf{Q}\mathbf{K}^T}{\sqrt{d}} + \log \mathbf{s} \right) \quad (1)$$

142 where \mathbf{s} is the number of patches the token represents after token merging. We conduct frame-wise
 143 token merging in AURORACAP, the visualization of token merging can be found in Appendix E.

144 2.2 TRAINING RECIPE

145 Building upon the exploration in works like Prismatic VLMs (Karamcheti et al., 2024),
 146 Idefics2 (Laurençon et al., 2024), and InternVL (Chen et al., 2023b), we further adopt a three-
 147 stage training strategy, which can be noted as Pretraining stage, Vision stage and Language stage. The
 148 training data used in each stage are shown in Table G6, Table G7 and Table G8. More training details
 149 including hyper-parameters selection and data preprocessing operation can be found in Appendix G.

150 **Pretraining stage.** Similar to LLaVA, we first align visual features from the vision encoder ViT with
 151 the word embedding space of LLMs. To achieve this, we freeze the pretrained ViT and LLM, training
 152 solely the vision-language connector. Consistent with LLaVA-1.5 (Li et al., 2024a), we employ
 153 a two-layer MLP as the projection layer and pretrain on 1.3M image-caption pairs. To optimize
 154 performance, we explore various combinations of the pre-trained ViT and LLM in Appendix F.

Table 2: Comparison of AURORACAP with LLM-based SoTA methods on image-captioning benchmarks under a zero-shot setting, **except k -shot where k is marked as a superscript**. The GPT-4V CIDEr results are from (Team, 2024), the only reference we know of, but seem oddly low. * marks fine-tuned results. Scores in **bold** indicate the best performance under zero-shot setting.

Model	Flickr (31,784)					NoCaps (4,500)					COCO-Cap (5,000)				
	CI-DEr	BLEU@1	BLEU@4	Met-eor	ROUGE	CI-DEr	BLEU@1	BLEU@4	Met-eor	ROUGE	CI-DEr	BLEU@1	BLEU@4	Met-eor	ROUGE
InstructBLIP-7B (Dai et al., 2024b)	78.2	77.1	30.9	24.8	53.4	118.2	88.2	47.2	30.3	62.0	141.3*	82.8*	41.7*	30.9*	61.0*
InstructBLIP-13B (Dai et al., 2024b)	76.1	76.8	30.1	24.4	53.0	116.3	88.3	46.7	29.8	61.4	135.0*	82.2*	39.7*	29.8*	59.8*
LLaVA-1.5-7B (Liu et al., 2023)	74.9	71.7	28.4	26.1	52.8	105.5	82.6	40.2	30.3	59.4	110.3	73.0	29.7	29.2	55.5
LLaVA-1.5-13B (Liu et al., 2023)	79.4	73.6	30.2	26.6	53.9	109.2	84.2	42.4	30.6	60.3	115.6	74.6	31.5	29.4	56.5
LLaVA-1.6-7B (Liu et al., 2024a)	68.4	69.6	26.6	23.2	50.3	88.4	73.8	34.8	25.9	54.6	99.9	67.7	28.4	25.5	52.4
LLaVA-1.6-13B (Liu et al., 2024a)	66.6	65.2	24.2	22.2	48.8	88.1	68.7	34.0	25.4	54.9	101.8	62.2	27.5	24.6	52.1
MiniCPM-V-3B (Hu et al., 2023)	66.8	68.0	25.1	27.2	51.0	89.9	79.1	33.2	29.7	55.8	94.2	69.8	23.9	28.3	52.3
DeCap (Li et al., 2023d)	56.7	—	21.2	21.8	—	42.7	—	—	—	—	91.2	—	24.7	25.0	—
Flamingo-80B (Alayrac et al., 2022)	67.2	—	—	—	—	—	—	—	—	—	84.3	—	—	—	—
Chameleon-34B (Team, 2024)	74.7 ²	—	—	—	—	—	—	—	—	—	120.2 ²	—	—	—	—
GPT-4V	55.3 ⁸	—	—	—	—	—	—	—	—	—	78.5 ⁸	—	—	—	—
Gemini-1.5 Pro	82.2 ⁴	—	—	—	—	—	—	—	—	—	99.8 ²	—	—	—	—
AURORACAP-7B	88.9	75.6	32.8	26.7	55.4	111.4	85.6	44.4	29.9	60.6	120.8	78.0	35.3	28.6	57.2

Vision stage. Unlike LLaVA, we next unfreeze the pretrained ViT while freezing the LLM during vision stage and train with the public data among various computer vision tasks (*e.g.*, captioning, object identification, classification, reasoning, VQA, *etc.*) to get better generalization (Huh et al., 2024). The motivation for doing this is that CLIP ViT usually performs poorly in aspects such as Orientation and Direction, Positional and Relational Context, Quantity and Count (Tong et al., 2024b). However, since the most of the collected datasets lack high-quality and detailed corresponding language descriptions, the labels often consist of only a few words or a short phrase when converted to text. Therefore, unfreezing the language model at this stage is risky, as it may lead to a degradation in the performance of the language model.

Language stage. Finally, we conduct end-to-end training, which means all the components are trainable, with the most high-quality public data during language stage training. We mix all the data, including images and videos, captions and instructions, into each mini-batch for training. To improve video captioning performance, we duplicate the video captioning datasets twice. We remove all the video training data for training a image-based AURORACAP as well for image captioning task.

2.3 EVALUATION

In this section we evaluate AURORACAP on various tasks including image captioning, video captioning, and video question answering. Appendix H show detailed evaluation settings.

Image Captioning. We evaluate AURORACAP using CIDEr (C), BLEU-4 (B@4), BLEU-1 (B@1), METEOR (M), and ROUGE-L (R) metric on Flickr (Plummer et al., 2015), NoCaps (Agrawal et al., 2019), and COCO-Cap (Lin et al., 2014) benchmarks and compare it with LLM-based state-of-the-art methods as shown in Table 2. We show the performance of image based AURORACAP under zero-shot settings. Notice that these benchmarks all contain short captions consisting of a single sentence, so they only partially reflect the model’s performance. The performance mentioned in the rest of this paper refers to video-based AURORACAP.

Video Captioning. Although the current video captioning benchmarks **only contain** one-sentence captions, to compare with prior work, we similarly evaluate on these benchmarks. We evaluate AURORACAP using CIDEr (C), BLEU-4 (B@4), BLEU-1 (B@1), METEOR (M), and ROUGE-L (R) metric on MSR-VTT (Xu et al., 2016), VATEX (Wang et al., 2019) as shown in Table 3.

Video Question Answering. We evaluate AURORACAP on MSVD-QA (Xu et al., 2017), ActivityNet-QA (Yu et al., 2019), MSRVTQA (Xu et al., 2017), and iVQA (Yang et al., 2021) for video question answering tasks as shown in Table 4. Although AURORACAP is primarily a captioning model, it achieves competitive performance in some VQA datasets (ANet, iVQA). For others (MSVD, MSR-VTT) performance is more modest, but still not bad. In some failure cases observed in the model, we found that prompting the model to generate a comprehensive caption for the video input can lead to outputs that include the correct answer. This phenomenon may be attributed to a disruption in the model’s instruction-following capabilities during the visual-based training period. We regard this as a promising avenue for future research.

Table 3: Comparison of AURORACAP with SoTA methods on existing video captioning benchmarks under zero-shot setting. AURORACAP substantially outperforms other recent methods.

Model	MSR-VTT (1,000)					VATEX (1,000)				
	CI-DEr	BLEU @1	BLEU @4	Met-eor	ROU-GE	CI-DEr	BLEU @1	BLEU @4	Met-eor	ROU-GE
ZeroCap (Tewel et al., 2022)	9.6	–	2.9	16.3	35.4	–	–	–	–	–
DeCap (Li et al., 2023d)	18.6	–	14.7	20.4	–	18.7	–	13.1	15.3	–
PaLI-3 (Chen et al., 2022)	21.3	–	–	–	–	–	–	–	–	–
Ma et al. (Ma et al., 2024)	22.1	–	3.5	17.3	28.7	23.9	–	2.8	14.1	23.5
LLaVA-7B (Liu et al., 2024b)	16.9	–	–	–	–	–	–	–	–	–
Video-LLaMA (Zhang et al., 2023a)	2.3	–	4.9	16.8	–	3.8	–	4.3	16.3	21.8
AURORACAP-7B	33.1	58.6	21.0	23.9	49.5	33.8	57.1	18.4	19.0	40.8

Table 4: Comparison of AURORACAP with SoTA methods on video question answering and classification benchmarks under zero-shot setting. The pretrained LLM size is 7B for all listed models.

Model	ANet		MSVD		MSR-VTT		iVQA
	Acc	Score	Acc	Score	Acc	Score	Acc
Just Ask (Yang et al., 2021)	–	–	–	–	–	–	12.2
FrozenBiLM (Yang et al., 2022)	24.7	–	32.2	–	16.8	–	26.8
Video-LLaMA (Zhang et al., 2023a)	12.4	1.1	51.6	2.5	29.6	1.8	–
VideoChat (Li et al., 2023b)	26.5	2.2	56.3	2.8	45.0	2.5	–
Video-ChatGPT (Maaz et al., 2023)	35.2	2.7	64.9	3.3	49.3	2.8	–
LLaMA-VID (Li et al., 2023g)	47.4	3.3	69.7	3.7	57.7	3.2	–
Video-LLaVA (Lin et al., 2023a)	45.3	3.3	70.7	3.9	59.2	3.5	–
FreeVA (Wu, 2024)	51.2	3.5	73.8	4.1	60.0	3.5	–
LLaVA-NeXT-Video (Liu et al., 2024a)	53.5	3.2	–	–	–	–	–
MovieChat (Song et al., 2023)	45.7	3.4	75.2	3.8	52.7	2.6	–
MovieChat+ (Song et al., 2024)	48.1	3.4	76.5	3.9	53.9	2.7	–
AURORACAP-7B	61.8	3.8	62.6	3.6	43.5	2.9	55.2

3 VDC: A VIDEO DETAILED CAPTIONING BENCHMARK

3.1 BENCHMARK DATASET CURATION

3.1.1 VIDEO COLLECTION AND PROCESSING

To ensure the reliability of the benchmark, it is crucial to maintain high video quality, balanced data distribution, and content complexity. Panda-70M (Chen et al., 2024e) offers a high-resolution, open-domain YouTube video dataset with diverse one-minute clips across wildlife, cooking, sports, news, TV shows, gaming, and 3D rendering, ideal for studying complex real-world scenarios. Additionally, a large volume of aesthetically appealing videos from user-uploaded platforms like Mixkit (Mixkit, 2024), Pixabay (Pixabay, 2024), and Pexels (Pexels, 2024) provides scenic views and visually pleasing human activities with minimal transitions and simpler events. Ego4D (Grauman et al., 2022) complements the video source by focusing on ego-centric human activities and auto-driving scenarios, ensuring comprehensive coverage of real-world scenes. To mitigate content homogeneity among these candidate videos and maintain diversity in the final dataset, inspired by ShareGPT4Video (Chen et al., 2024d), we building VDC upon those various video sources. Note that the videos used in VDC construction are not included in the training data of AURORACAP. To ensure balanced data distribution, we allocate equal proportions of videos from Panda-70M (Chen et al., 2024e), Ego4D (Grauman et al., 2022), Mixkit (Mixkit, 2024), Pixabay (Pixabay, 2024), and Pexels (Pexels, 2024). We first split the video into clips and apply dense frame extraction.

3.1.2 STRUCTURED DETAILED CAPTIONS CONSTRUCTION PIPELINE

We believe that a comprehensive detailed video caption benchmark should encompass various aspects, including main objects, camera movements, and background. However, most existing benchmarks (Li et al., 2024b; Chen et al., 2024d) provide only a single caption for the entire video with less structured

Table 5: The video source distribution of the proposed VDC benchamrk including diverse settings such as natural landscapes, human activities, and animal activities. Videos from different sources have a similar proportion in VDC, reducing the data bias.

Video Source	# Sample	Proportion	Duration (sec.)	Ave. Length (sec.)	Ave. # Keyframe
Panda-70M (Chen et al., 2024e)	229	22.25%	5,714	24.95	7.18
Ego4D (Grauman et al., 2022)	196	19.05%	10,935	55.79	19.46
Mixkit (Mixkit, 2024)	197	19.14%	3,261	16.55	6.58
Pixabay (Pixabay, 2024)	199	19.34%	4,748	23.86	8.99
Pexels (Pexels, 2024)	208	20.21%	4,343	20.88	7.99
Total	1,027	—	29,001	28.18	10.43

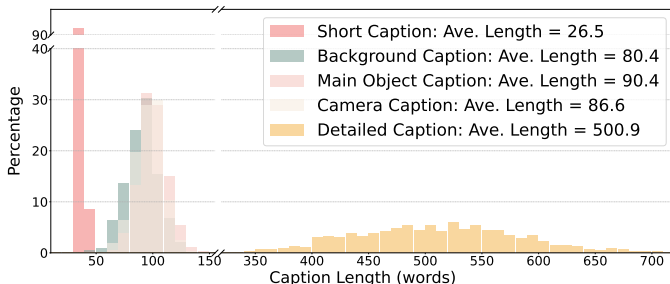
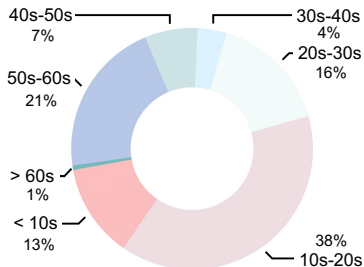


Figure 1: Video length statistics.

Figure 2: Distribution of structured caption length.

details. Therefore, we develop a structured detailed captions construction pipeline to generate extra detailed descriptions from various perspectives, significantly extending the length and enhancing the richness compared to previous benchmarks. Following (Ju et al., 2024), the structured captions in VDC encompass not only **short** and **detailed captions** but also three additional categories: (1) **main object caption**, offering a comprehensive analysis of the primary subjects’ actions, attributes, interactions, and movements across frames, including variations in posture, expression, and speed; (2) **background caption**, providing detailed descriptions of the background, such as objects, location, weather, time, and dynamic elements; and (3) **camera caption**, which details the camera work, including shot types, angles, movements, transitions, and special effects.

To generate detailed, fine-grained, and accurate captions, we leverage GPT-4o to produce video descriptions. We utilize the dense video frames to obtain captions. We observed that generating all captions in a single conversation round often introduces hallucinations in the detailed captions. To address this, we design a hierarchical prompt strategy to efficiently obtain accurate structured captions and detailed captions in two conversation rounds: (1) structured captions generation and (2) detailed captions integration. In the first round, the prompt briefly introduces the differences between structured captions and uses the dense video frames as input to generate the short caption, main object caption, background caption, camera caption, and the detailed caption. In the second round, the generated captions serve as the reference. The second-round prompt guides GPT-4o to enhance the detailed caption based on the initial captions, ensuring consistency without introducing new entities or relations, and producing a vivid, engaging, and informative description. The whole prompt template for the structured detailed captions construction pipeline can be found in Appendix K. Finally, we conduct a manual review to correct captions with hallucinations and supplement omitted visual elements. The refined detail structured captions are then used as the ground truth for evaluation.

3.1.3 COMPARISON ON NUMERICAL STATISTICS

Based on the hierarchical scheme, VDC can capture a rich variety of details of the video and reduce hallucinations. The visual representation in Figure 1 demonstrates the video duration distribution of VDC. Over 87% of the videos exhibit a duration ranging from 10K to 12K frames, while 1% of videos extending beyond 60 seconds. Only 13% of videos have duration less than 10 seconds. As illustrated in Table 1, the average length of detailed descriptions in VDC is significantly longer than in previous benchmarks. Figure 2 shows the length distribution of structured captions in VDC, with detailed captions averaging over 500 words. Appendix M present more statistics.

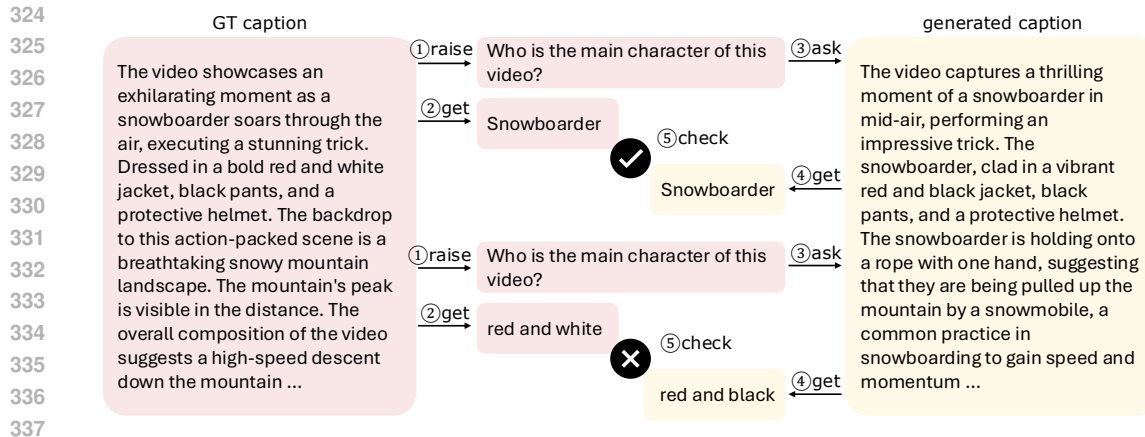


Figure 3: Evaluation pipeline with VDCSCORE. Like when humans take reading comprehension tests, we transform the matching between two paragraphs into a set of question-answer pairings. We first generate some question-answer pairs based on the ground truth captions, then derive corresponding answers one by one from the generated captions, and finally perform matching. The process is automatically evaluated with the LLM involvement in each step.

3.2 EVALUATION METRIC DESIGN AND LEADERBOARD

3.2.1 VDCSCORE: EVALUATING DETAILED CAPTIONS WITH LLMs

Evaluating video captions requires not only assessing the quality of the captions but also flexibly evaluating the alignment between the video and the caption. While metrics such as BLEU (Papineni et al., 2002), CIDEr (Vedantam et al., 2015), and ROUGE-L (Lin, 2004) have been employed for caption evaluation, these metrics are predominantly designed for short captions and rely heavily on word-level frequency-based alignment. Given the advanced semantic understanding capabilities of large language models (LLMs), Video-ChatGPT (Li et al., 2023b) proposes using LLM as an evaluation assistant to directly judge the correctness of the whole predicted captions and assign scores. However, as demonstrated in Table 6, our experiments indicate that when dealing with detailed captions, the direct application of LLM struggles to accurately distinguish the correctness of various predicted captions, fails to effectively evaluate the precision of detailed descriptions, and exhibits a tendency to assign disproportionately lower scores. Therefore, we introduce VDCSCORE, a novel quantitative metric that utilizes LLMs to evaluate the similarity between predicted and ground-truth detailed captions through a divide-and-conquer approach.

The core idea of VDCSCORE is to decompose long detailed captions into multiple short question-answering pairs, average the evaluation of each pair as the final result. We elaborate the design of VDCSCORE in the following parts: (1) ground-truth question-answer pairs extraction, (2) responded answers generation and (3) answers matching. As illustrated in Figure 3, we first employ GPT-4o¹ to generate question-answer pairs from the detailed ground-truth caption. To ensure that the generated question-answer pairs capture as much information as possible from the original caption and facilitate accurate evaluation by LLMs, we constrain the number of generated pairs and impose specific guidelines: the questions must be open-ended, and the answers should be concise, and directly relevant to the questions. For a fair comparison and to mitigate potential variability arising from generating different question-answer pairs for the same caption, we pre-generate a standardized set of question-answer pairs for all captions in VDC, as depicted in Figure 3. The used prompt templates used along with additional examples, are provided in Appendix L.

VDCSCORE subsequently analyzes the predicted captions by leveraging ground-truth question-answer pairs. We prompt GPT-4o to read the detailed predicted captions and generate answers based solely on these captions. To mitigate biases arising from discrepancies in the length between ground-truth and predicted answers, we also impose constraints ensuring that responses are limited to concise sentences or phrases. Consequently, for each pair of ground-truth and predicted captions, we

¹GPT-4o latest version in September, 2024.

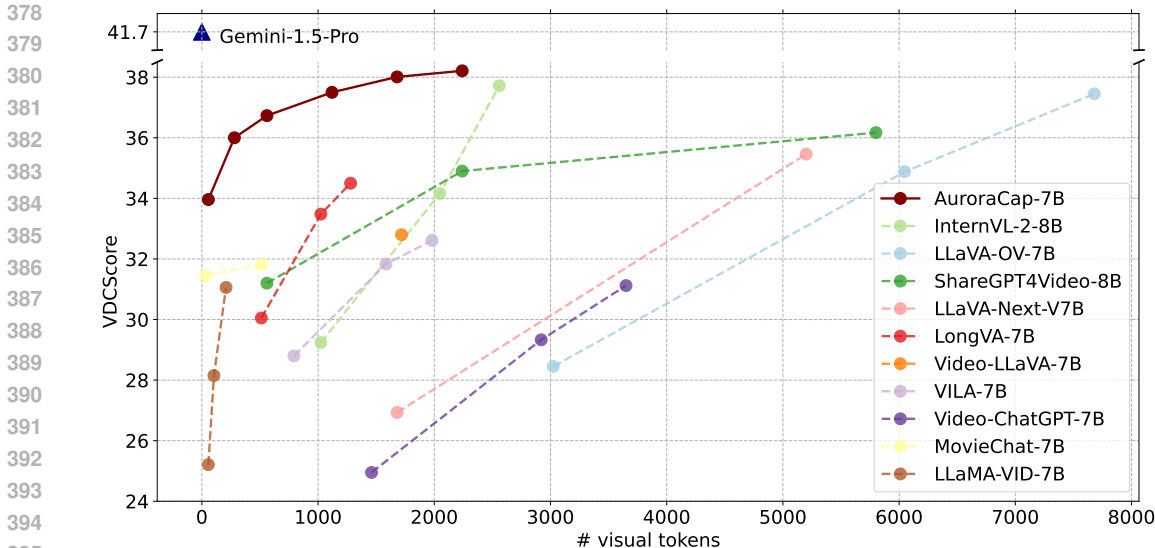


Figure 4: Comparison between various models with different number of visual tokens input on VDC. For Gemini-1.5-Pro, we only report the performance. We manage the number of visual tokens by managing token merging for AURORACAP, and manage the number of frames for others. AURORACAP achieves a much better VDCSCORE than all other models given a certain compression in the number of visual tokens kept and indeed approaches the performance of Gemini-1.5-Pro.

Table 6: Comparison of AURORACAP with LLM-based baseline methods on VDCSCORE and other evaluation metrics under zero-shot setting. For each evaluation metric, we report the average value of the five structured captions in VDC. Note that VDD, CIDEr, and BLEU are only the average of background and main object caption, since the values of the others are closed to zero.

Model	VDCSCORE		VDD		CI-DEr	BLEU @1	BLEU @4	Met-eor	ROU-GE	Elo
	Acc	Score	Acc	Score						
Gemini-1.5 Pro (Reid et al., 2024)	41.73	2.15	49.68	3.07	5.97	29.72	2.63	21.21	20.19	1,171
LLaMA-VID (Li et al., 2023f)	30.86	1.62	4.63	1.63	1.48	17.74	1.46	8.07	17.47	859
Video-ChatGPT-7B (Maaz et al., 2023)	31.12	1.62	8.57	1.84	2.92	17.31	2.19	11.57	16.96	944
MovieChat-7B (Song et al., 2023)	31.92	1.64	10.24	1.86	5.14	14.33	3.17	13.60	14.98	890
VILA-7B (Lin et al., 2023b)	32.61	1.70	16.27	2.02	8.20	19.13	2.11	5.62	16.63	1,073
Video-LLaVA-7B (Lin et al., 2023a)	32.80	1.72	14.14	2.00	4.43	17.20	2.32	10.36	17.53	1,007
LLaVA-1.5-7B (Liu et al., 2023)	33.98	1.76	26.71	2.33	6.63	29.80	2.54	22.79	20.36	825
LongVA-7B (Zhang et al., 2024b)	34.50	1.79	32.65	2.69	4.83	18.75	2.16	13.43	14.84	969
LLaVA-1.5-13B (Liu et al., 2023)	34.78	1.80	28.26	2.36	3.90	20.43	2.02	26.37	17.87	943
LLaVA-NeXT-V7B (Zhang et al., 2024d)	35.46	1.85	25.62	2.34	2.66	20.18	2.33	28.17	17.51	1,022
LLaVA-1.6-7B (Liu et al., 2024a)	35.70	1.85	40.16	2.69	3.09	17.36	1.59	24.23	17.08	846
LLaVA-1.6-13B (Liu et al., 2024a)	35.85	1.85	34.55	2.51	5.55	29.23	2.50	20.26	19.96	728
ShareGPT4Video-8B (Chen et al., 2024d)	36.17	1.85	36.44	1.85	1.02	12.61	0.79	8.33	16.31	1,102
LLaVA-OV-7B (Li et al., 2024a)	37.45	1.94	41.83	2.70	4.09	28.34	2.84	23.98	19.59	1,155
InternVL-2-8B (Chen et al., 2023b)	37.72	1.96	48.99	3.03	5.59	15.75	2.48	10.76	17.63	1,081
AURORACAP-7B	38.21	1.98	48.33	2.90	9.51	30.90	4.06	19.09	21.58	1,267

obtain a set of <question, correct answer, predicted answer> triplets. Following Video-ChatGPT (Li et al., 2023b), we then ask GPT-4o to output two scores for each triplet: one for answer correctness and another for answer quality. The final accuracy and score are calculated by averaging the correctness score and quality score respectively. When using two same captions as input, VDCSCORE returns an accuracy of 100%, demonstrating the feasibility and reliability.

3.2.2 BENCHMARKING VIDEO DETAILED CAPTIONING

To our knowledge, no standard evaluation benchmarks have been established for detailed video captioning. To advance this field, we assess several baselines on our proposed VDC. As illustrated in Table 6, we present a quantitative comparison between our AURORACAP with existing state-of-the-art LMMs. We compare the VDCSCORE with both rule-based and model-based caption metrics with AURORACAP performing well. BLEU (Papineni et al., 2002), CIDEr (Vedantam et al.,

Table 7: Comparison of AURORACAP with LLM-based baseline methods on VDCSCORE under zero-shot structured captions setting. We consider the VDCSCORE of detailed captions, short captions, background captions, main object captions and camera captions. We also test the vision-blind case suggesting by (Chen et al., 2024c; Tong et al., 2024a).

Model	Camera Acc / Score	Short Acc / Score	Background Acc / Score	Main Object Acc / Score	Detailed Acc / Score
Vicuna-v1.5-7B (Chiang et al., 2023)	21.68 / 1.12	23.06 / 1.17	22.02 / 1.15	22.64 / 1.16	23.09 / 1.20
Llama-3.1-8B (Dubey et al., 2024)	17.83 / 1.00	17.90 / 1.02	19.52 / 1.10	19.57 / 1.10	20.10 / 1.22
Gemini-1.5 Pro (Reid et al., 2024)	38.68 / 2.05	35.71 / 1.85	43.84 / 2.23	47.32 / 2.41	43.11 / 2.22
LLaMA-VID (Li et al., 2023f)	39.47 / 2.10	29.92 / 1.56	28.01 / 1.45	31.24 / 1.59	25.67 / 1.38
Video-ChatGPT-7B (Maaz et al., 2023)	37.46 / 2.00	29.36 / 1.56	33.68 / 1.70	30.47 / 1.60	24.61 / 1.26
MovieChat-7B (Song et al., 2023)	37.25 / 1.98	32.55 / 1.59	28.99 / 1.54	31.97 / 1.64	28.82 / 1.46
VILA-7B (Lin et al., 2023b)	34.33 / 1.83	30.40 / 1.55	35.15 / 1.80	33.38 / 1.72	29.78 / 1.58
Video-LLaVA-7B (Lin et al., 2023a)	37.48 / 1.97	30.67 / 1.63	32.50 / 1.70	36.01 / 1.85	27.36 / 1.43
LLaVA-1.5-7B (Liu et al., 2023)	38.38 / 2.04	28.61 / 1.51	34.86 / 1.79	34.62 / 1.76	33.43 / 1.73
LongVA-7B (Zhang et al., 2024b)	35.32 / 1.90	31.94 / 1.63	36.39 / 1.85	40.95 / 2.11	27.91 / 1.48
LLaVA-1.5-13B (Liu et al., 2023)	38.97 / 2.07	30.89 / 1.60	34.79 / 1.78	36.27 / 1.84	33.00 / 1.74
LLaVA-NeXT-V7B (Zhang et al., 2024d)	39.73 / 2.10	30.63 / 1.60	36.54 / 1.88	36.54 / 1.88	33.84 / 1.77
LLaVA-1.6-7B (Liu et al., 2024a)	36.50 / 1.93	31.91 / 1.65	37.58 / 1.92	36.03 / 1.85	36.47 / 1.89
LLaVA-1.6-13B (Liu et al., 2024a)	35.61 / 1.86	31.90 / 1.66	38.90 / 1.99	36.65 / 1.87	36.18 / 1.89
ShareGPT4Video-8B (Chen et al., 2024d)	33.28 / 1.76	39.08 / 1.94	35.77 / 1.81	37.12 / 1.89	35.62 / 1.84
LLaVA-OV-7B (Li et al., 2024a)	37.82 / 2.02	32.58 / 1.70	37.43 / 1.92	38.21 / 1.96	41.20 / 2.13
InternVL-2-8B (Chen et al., 2023b)	39.08 / 2.11	33.02 / 1.74	37.47 / 1.89	44.16 / 2.22	34.89 / 1.82
AURORACAP-7B	43.50 / 2.27	32.07 / 1.68	35.92 / 1.84	39.02 / 1.97	41.30 / 2.15

Table 8: Comparison of AURORACAP with LLM-based baseline methods on VDD (Liu et al., 2024a) under zero-shot structured captions setting. We consider the VDD (Liu et al., 2024a) of detailed captions, short captions, background captions, main object captions and camera captions.

Model	Camera Acc / Score	Short Acc / Score	Background Acc / Score	Main Object Acc / Score	Detailed Acc / Score
Gemini-1.5 Pro (Reid et al., 2024)	18.89 / 2.115	16.91 / 1.572	57.73 / 3.263	41.64 / 2.886	2.581 / 0.330
LLaMA-VID (Li et al., 2023f)	28.28 / 2.513	1.034 / 1.042	6.198 / 1.895	3.063 / 1.366	2.046 / 0.304
Video-ChatGPT-7B (Maaz et al., 2023)	16.00 / 2.175	4.173 / 1.032	14.14 / 2.273	3.001 / 1.423	1.038 / 0.192
VILA-7B (Lin et al., 2023b)	4.005 / 1.751	2.087 / 0.233	22.45 / 2.385	10.10 / 1.672	1.015 / 0.262
Video-LLaVA-7B (Lin et al., 2023a)	20.00 / 2.336	3.193 / 1.064	17.17 / 2.253	11.11 / 1.765	3.130 / 0.316
LLaVA-1.5-7B (Liu et al., 2023)	26.88 / 2.515	1.222 / 0.793	36.50 / 2.725	16.92 / 1.937	0.694 / 0.276
LongVA-7B (Zhang et al., 2024b)	17.00 / 2.204	1.016 / 0.794	50.00 / 3.203	15.31 / 2.196	0.002 / 0.247
LLaVA-1.5-13B (Liu et al., 2023)	32.65 / 2.662	2.836 / 0.922	37.55 / 2.749	18.98 / 1.978	0.688 / 0.275
LLaVA-NeXT-V7B (Zhang et al., 2024d)	29.81 / 2.645	1.913 / 0.957	33.23 / 2.692	18.02 / 1.999	0.887 / 0.279
LLaVA-1.6-7B (Liu et al., 2024a)	21.11 / 2.229	8.696 / 1.146	53.31 / 3.105	27.01 / 2.286	1.282 / 0.279
LLaVA-1.6-13B (Liu et al., 2024a)	21.56 / 2.199	9.798 / 1.206	39.37 / 2.692	29.73 / 2.329	1.287 / 0.271
ShareGPT4Video-8B (Chen et al., 2024d)	33.28 / 1.768	4.908 / 0.986	35.77 / 1.813	37.12 / 1.899	3.213 / 0.752
LLaVA-OV-7B (Li et al., 2024a)	17.11 / 2.086	11.15 / 1.277	55.82 / 3.149	27.84 / 2.258	1.372 / 0.249
InternVL-2-8B (Chen et al., 2023b)	29.00 / 2.545	4.041 / 1.079	63.64 / 3.446	34.34 / 2.627	3.032 / 0.394
AURORACAP-7B	49.40 / 3.141	3.313 / 0.886	59.52 / 3.261	37.14 / 2.533	1.275 / 0.295

2015), ROUGE-L (Lin, 2004) and METEOR (Banerjee & Lavie, 2005) are included as representative rule-based metrics. For model-based metrics, we also consider Video Detailed Description (Li et al., 2023b) (VDD), which employs ChatGPT as an evaluation assistant to compare full captions.

Table 7 presents VDCSCORE performance across various sections of structured captions within VDC. Following (Chen et al., 2024c), we also incorporate vision-blind baselines. Furthermore, Figure 4 illustrates a schematic diagram of the performance and efficiency of different video training models. Since the comparison of model inference time under different architectures, models, deployment frameworks, and output lengths is unfair, so we used the number of visual tokens as a representation of efficiency. AURORACAP achieves superior performance in video detailed captioning while utilizing significantly fewer visual tokens than other models, fully highlighting the efficiency of AURORACAP. We also show additional experimental results with VDD metric as shown in Table 8. We also perform a human study using Elo ranking to supplement our evaluation and provide a more intuitive assessment of AURORACAP’s performance. As depicted in Figure 5, VDCSCORE shows better correlation with human evaluation results than VDD and ROUGE metric.

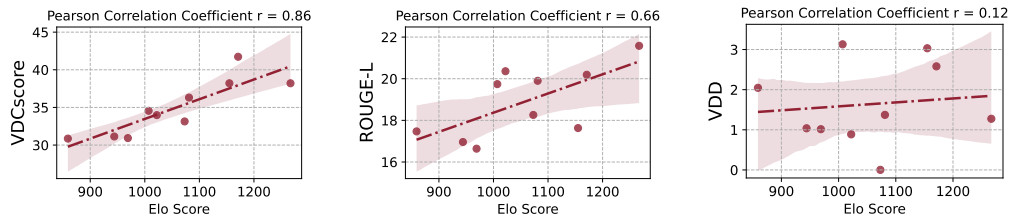


Figure 5: Pearson correlation analysis among three evaluation metrics—VDCSCORE, ROUGE-L (Lin, 2004), VDD (Liu et al., 2024a)—and human Elo rankings for video models. VDD reflects the score for detailed captions. VDCSCORE demonstrates the highest consistency with expert judgments, thereby reinforcing the reliability. The detailed settings are provided in the Appendix O.

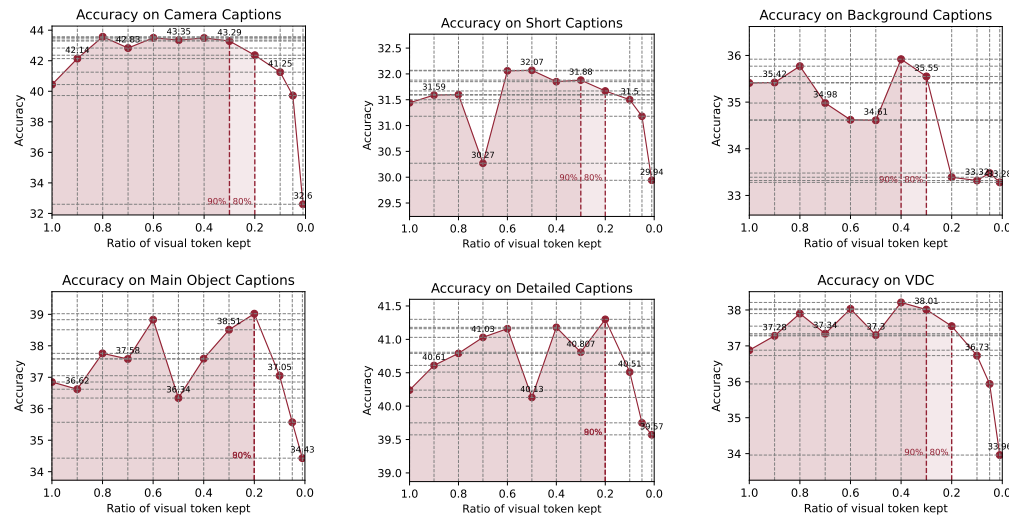


Figure 6: Ablation study of token merging on VDC. We found that token merging significantly reduces the number of tokens while maintaining minimal performance drop, and even showing improvement in some aspects. We highlight the token merging ratio when achieving 90% and 80% performance with the dash line and filled area.

Ablation study on token merging ratio. As a core strategy of AURORACAP, token merging plays a significant role in reducing the number of visual tokens. We further study how the video detailed captioning capability is influenced by token merge ratio. We define the performance percentage as the proportion between the highest and lowest values on the entire performance curve. As shown in Figure 6, most models maintain satisfactory performance ($> 80\%$) even with only 0.2 of visual token kept ratio. Since AURORACAP focuses on spatial visual token merging, the temporal features introduce additional complexity to explore the token merging laws, resulting in the optimal performance may occurs at a middle level of visual token kept ratio.

4 CONCLUSION

In this paper, we first introduce AURORACAP, a efficient video detailed captioner based on large multimodal model. By leveraging the token merging strategy, we significantly reduce the computational overhead without compromising performance. We also present VDC, a novel video detailed captioning benchmark designed to evaluate comprehensive and coherent textual descriptions of video content. For better evaluating, We propose VDCSCORE, a new LLM-assisted metric with divide-and-conquer strategy. Our extensive evaluation on various video and image captioning benchmarks demonstrated that AURORACAP achieves competitive results, even outperforming state-of-the-art models in some tasks. We also conduct thorough ablation studies to validate the effectiveness of token merging and other aspects of our model. We found that the current model performs poorly in terms of the trade-off between performance and the scale of input tokens. Additionally, there is still room for improvement in camera handling and detailed captioning.

540
541
542
543
544
545
546
547
548
549
550
551
552
553
554
555
556
557
558
559
560
561
562
563
564
565
566
567
568
569
570
571
572
573
574
575
576
577
578
579
580
581
582
583
584
585
586
587
588
589
590
591
592
593

ETHICS STATEMENT

This research on video captioning utilizes publicly available datasets, ensuring that all data complies with privacy regulations. We acknowledge the potential biases that can arise in automatic caption generation, particularly concerning gender, race, or other characteristics. We have taken measures to evaluate and minimize such biases, while remaining committed to further improvements. Additionally, we recognize the potential risks of misuse, such as generating misleading captions, and have checked the training dataset with safeguards against such applications.

REPRODUCIBILITY STATEMENT

We have made several efforts to ensure the reproducibility of our work. All the key implementation details, including the architecture of our model, the training procedures, and hyperparameter settings, are described in supplementary material Section [G](#). The introduction of the used evaluation benchmarks and settings are in Section [H](#). The introduction of the used evaluation benchmarks and settings are in Section [H](#). Prompt template of VDC generation is in Section [K](#). Question-answer pairs generation prompt template of VDCSCORE is in Section [L](#). And calculation details of Elo ranking is in Section [O](#). We have also outlined any hardware configurations and computation requirement used for our experiments in Figure [F8](#) to further support reproducibility. [The code for model training, evaluation, deployment, as well as model weight, benchmark, and training dataset of all the training stages will be released with the paper.](#)

REFERENCES

- 594
595
596 Harsh Agrawal, Karan Desai, Yufei Wang, Xinlei Chen, Rishabh Jain, Mark Johnson, Dhruv Batra,
597 Devi Parikh, Stefan Lee, and Peter Anderson. Nocaps: Novel object captioning at scale. In
598 *Proceedings of the IEEE/CVF international conference on computer vision*, pp. 8948–8957, 2019.
599 4, 32, 37
- 600 Jean-Baptiste Alayrac, Jeff Donahue, Pauline Luc, Antoine Miech, Iain Barr, Yana Hasson, Karel
601 Lenc, Arthur Mensch, Katherine Millican, Malcolm Reynolds, et al. Flamingo: a visual language
602 model for few-shot learning. *Advances in neural information processing systems*, 35:23716–23736,
603 2022. 4
- 604 Peter Anderson, Basura Fernando, Mark Johnson, and Stephen Gould. Spice: Semantic propositional
605 image caption evaluation. In *Computer Vision—ECCV 2016: 14th European Conference, Amster-*
606 *dam, The Netherlands, October 11–14, 2016, Proceedings, Part V 14*, pp. 382–398. Springer, 2016.
607 23
- 608 Jacob Andreas, Marcus Rohrbach, Trevor Darrell, and Dan Klein. Neural module networks. In
609 *Proceedings of the IEEE conference on computer vision and pattern recognition*, pp. 39–48, 2016.
610 34
- 611 Max Bain, Arsha Nagrani, Gül Varol, and Andrew Zisserman. Frozen in time: A joint video and
612 image encoder for end-to-end retrieval. In *Proceedings of the IEEE/CVF International Conference*
613 *on Computer Vision*, pp. 1728–1738, 2021. 2
- 614 Satanjeev Banerjee and Alon Lavie. Meteor: An automatic metric for mt evaluation with improved
615 correlation with human judgments. In *Proceedings of the acl workshop on intrinsic and extrinsic*
616 *evaluation measures for machine translation and/or summarization*, pp. 65–72, 2005. 2, 9
- 617 Omer Bar-Tal, Hila Chefer, Omer Tov, Charles Herrmann, Roni Paiss, Shiran Zada, Ariel Ephrat,
618 Junhwa Hur, Yuanzhen Li, Tomer Michaeli, et al. Lumiere: A space-time diffusion model for
619 video generation. *arXiv preprint arXiv:2401.12945*, 2024. 1
- 620 Lucas Beyer, Andreas Steiner, André Susano Pinto, Alexander Kolesnikov, Xiao Wang, Daniel
621 Salz, Maxim Neumann, Ibrahim Alabdulmohsin, Michael Tschannen, Emanuele Bugliarello, et al.
622 Paligemma: A versatile 3b vlm for transfer. *arXiv preprint arXiv:2407.07726*, 2024. 23
- 623 Ali Furkan Biten, Ruben Tito, Andres Mafla, Lluís Gomez, Marçal Rusinol, Ernest Valveny, CV Jawa-
624 har, and Dimosthenis Karatzas. Scene text visual question answering. In *Proceedings of the*
625 *IEEE/CVF international conference on computer vision*, pp. 4291–4301, 2019. 34
- 626 Daniel Bolya, Cheng-Yang Fu, Xiaoliang Dai, Peizhao Zhang, Christoph Feichtenhofer, and Judy
627 Hoffman. Token merging: Your ViT but faster. In *The Eleventh International Conference on*
628 *Learning Representations*, 2022. 2, 3
- 629 Fabian Caba Heilbron, Victor Escorcia, Bernard Ghanem, and Juan Carlos Niebles. Activitynet:
630 A large-scale video benchmark for human activity understanding. In *Proceedings of the ieee*
631 *conference on computer vision and pattern recognition*, pp. 961–970, 2015. 2, 23
- 632 Mu Cai, Jianwei Yang, Jianfeng Gao, and Yong Jae Lee. Matryoshka multimodal models. *arXiv*
633 *preprint arXiv:2405.17430*, 2024. 23
- 634 Wenhao Chai, Xun Guo, Gaoang Wang, and Yan Lu. Stablevideo: Text-driven consistency-aware
635 diffusion video editing. In *Proceedings of the IEEE/CVF International Conference on Computer*
636 *Vision*, pp. 23040–23050, 2023. 1
- 637 David Chen and William B Dolan. Collecting highly parallel data for paraphrase evaluation. In
638 *Proceedings of the 49th annual meeting of the association for computational linguistics: human*
639 *language technologies*, pp. 190–200, 2011. 2, 23
- 640 Guiming Hardy Chen, Shunian Chen, Ruifei Zhang, Junying Chen, Xiangbo Wu, Zhiyi Zhang,
641 Zhihong Chen, Jianquan Li, Xiang Wan, and Benyou Wang. Allava: Harnessing gpt4v-synthesized
642 data for a lite vision-language model. *arXiv preprint arXiv:2402.11684*, 2024a. 34

- 648 Liang Chen, Haozhe Zhao, Tianyu Liu, Shuai Bai, Junyang Lin, Chang Zhou, and Baobao Chang.
649 An image is worth 1/2 tokens after layer 2: Plug-and-play inference acceleration for large vision-
650 language models. *arXiv preprint arXiv:2403.06764*, 2024b. [2](#)
651
- 652 Lin Chen, Jisong Li, Xiaoyi Dong, Pan Zhang, Conghui He, Jiaqi Wang, Feng Zhao, and Dahua
653 Lin. Sharegpt4v: Improving large multi-modal models with better captions. *arXiv preprint*
654 *arXiv:2311.12793*, 2023a. [34](#)
- 655 Lin Chen, Jinsong Li, Xiaoyi Dong, Pan Zhang, Yuhang Zang, Zehui Chen, Haodong Duan, Jiaqi
656 Wang, Yu Qiao, Dahua Lin, et al. Are we on the right way for evaluating large vision-language
657 models? *arXiv preprint arXiv:2403.20330*, 2024c. [9](#)
658
- 659 Lin Chen, Xilin Wei, Jinsong Li, Xiaoyi Dong, Pan Zhang, Yuhang Zang, Zehui Chen, Haodong
660 Duan, Bin Lin, Zhenyu Tang, et al. Sharegpt4video: Improving video understanding and generation
661 with better captions. *arXiv preprint arXiv:2406.04325*, 2024d. [2](#), [5](#), [8](#), [9](#), [30](#), [34](#)
662
- 663 Tsai-Shien Chen, Aliaksandr Siarohin, Willi Menapace, Ekaterina Deyneka, Hsiang-wei Chao,
664 Byung Eun Jeon, Yuwei Fang, Hsin-Ying Lee, Jian Ren, Ming-Hsuan Yang, et al. Panda-70m:
665 Captioning 70m videos with multiple cross-modality teachers. In *Proceedings of the IEEE/CVF*
666 *Conference on Computer Vision and Pattern Recognition*, pp. 13320–13331, 2024e. [5](#), [6](#)
- 667 Xi Chen, Xiao Wang, Soravit Changpinyo, AJ Piergiovanni, Piotr Padlewski, Daniel Salz, Sebastian
668 Goodman, Adam Grycner, Basil Mustafa, Lucas Beyer, et al. Pali: A jointly-scaled multilingual
669 language-image model. *arXiv preprint arXiv:2209.06794*, 2022. [5](#)
670
- 671 Xin Chen, Yu Zhu, Hua Zhou, Liang Diao, and Dongyan Wang. Chinesefoodnet: A large-scale image
672 dataset for chinese food recognition. *arXiv preprint arXiv:1705.02743*, 2017. [34](#)
- 673 Zhe Chen, Jiannan Wu, Wenhai Wang, Weijie Su, Guo Chen, Sen Xing, Zhong Muyan, Qinglong
674 Zhang, Xizhou Zhu, Lewei Lu, et al. InternVL: Scaling up vision foundation models and aligning
675 for generic visual-linguistic tasks. *arXiv preprint arXiv:2312.14238*, 2023b. [1](#), [3](#), [8](#), [9](#)
676
- 677 Zesen Cheng, Sicong Leng, Hang Zhang, Yifei Xin, Xin Li, Guanzheng Chen, Yongxin Zhu, Wenqi
678 Zhang, Ziyang Luo, Deli Zhao, et al. Videollama 2: Advancing spatial-temporal modeling and
679 audio understanding in video-llms. *arXiv preprint arXiv:2406.07476*, 2024. [23](#)
- 680 Wei-Lin Chiang, Zhuohan Li, Zi Lin, Ying Sheng, Zhanghao Wu, Hao Zhang, Lianmin Zheng,
681 Siyuan Zhuang, Yonghao Zhuang, Joseph E Gonzalez, et al. Vicuna: An open-source chatbot
682 impressing gpt-4 with 90%* chatgpt quality. See <https://vicuna.lmsys.org> (accessed 14 April
683 2023), 2(3):6, 2023. [9](#)
684
- 685 Dawei Dai, YuTang Li, YingGe Liu, Mingming Jia, Zhang YuanHui, and Guoyin Wang. 15m mul-
686 timodal facial image-text dataset, 2024a. URL <https://arxiv.org/abs/2407.08515>.
687 [34](#)
- 688 Wenliang Dai, Junnan Li, Dongxu Li, Anthony Meng Huat Tiong, Junqi Zhao, Weisheng Wang,
689 Boyang Li, Pascale N Fung, and Steven Hoi. Instructblip: Towards general-purpose vision-
690 language models with instruction tuning. *Advances in Neural Information Processing Systems*, 36,
691 2024b. [1](#), [4](#)
692
- 693 Abhishek Das, Satwik Kottur, Khushi Gupta, Avi Singh, Deshraj Yadav, José MF Moura, Devi Parikh,
694 and Dhruv Batra. Visual dialog. In *Proceedings of the IEEE conference on computer vision and*
695 *pattern recognition*, pp. 326–335, 2017. [34](#)
- 696 Jie Deng, Wenhao Chai, Jianshu Guo, Qixuan Huang, Wenhao Hu, Jenq-Neng Hwang, and
697 Gaoang Wang. Citygen: Infinite and controllable 3d city layout generation. *arXiv preprint*
698 *arXiv:2312.01508*, 2023. [1](#)
699
- 700 Jie Deng, Wenhao Chai, Junsheng Huang, Zhonghan Zhao, Qixuan Huang, Mingyan Gao, Jianshu
701 Guo, Shengyu Hao, Wenhao Hu, Jenq-Neng Hwang, et al. Citycraft: A real crafter for 3d city
generation. *arXiv preprint arXiv:2406.04983*, 2024. [1](#)

- 702 Alexey Dosovitskiy, Lucas Beyer, Alexander Kolesnikov, Dirk Weissenborn, Xiaohua Zhai, Thomas
703 Unterthiner, Mostafa Dehghani, Matthias Minderer, Georg Heigold, Sylvain Gelly, et al. An image
704 is worth 16x16 words: Transformers for image recognition at scale. In *International Conference
705 on Learning Representations*, 2020. 1
- 706 Yilun Du, Sherry Yang, Bo Dai, Hanjun Dai, Ofir Nachum, Josh Tenenbaum, Dale Schuurmans, and
707 Pieter Abbeel. Learning universal policies via text-guided video generation. *Advances in Neural
708 Information Processing Systems*, 36, 2024. 1
- 709 Zhengfang Duanmu, Wentao Liu, Zhongling Wang, and Zhou Wang. Quantifying visual image
710 quality: A bayesian view. *Annual Review of Vision Science*, 7:437–464, 2021. 34
- 711 Abhimanyu Dubey, Abhinav Jauhri, Abhinav Pandey, Abhishek Kadian, Ahmad Al-Dahle, Aiesha
712 Letman, Akhil Mathur, Alan Schelten, Amy Yang, Angela Fan, et al. The llama 3 herd of models.
713 *arXiv preprint arXiv:2407.21783*, 2024. 9
- 714 Desmond Elliott, Stella Frank, Khalil Sima’an, and Lucia Specia. Multi30k: Multilingual english-
715 german image descriptions. *arXiv preprint arXiv:1605.00459*, 2016. 34
- 716 Chaoyou Fu, Yuhan Dai, Yondong Luo, Lei Li, Shuhuai Ren, Renrui Zhang, Zihan Wang, Chenyu
717 Zhou, Yunhang Shen, Mengdan Zhang, et al. Video-mme: The first-ever comprehensive evaluation
718 benchmark of multi-modal llms in video analysis. *arXiv preprint arXiv:2405.21075*, 2024. 2
- 719 Haoyuan Gao, Junhua Mao, Jie Zhou, Zhiheng Huang, Lei Wang, and Wei Xu. Are you talking to a
720 machine? dataset and methods for multilingual image question. *Advances in neural information
721 processing systems*, 28, 2015. 34
- 722 Roopal Garg, Andrea Burns, Burcu Karagol Ayan, Yonatan Bitton, Ceslee Montgomery, Yasumasa
723 Onoe, Andrew Bunner, Ranjay Krishna, Jason Baldridge, and Radu Soricut. Imageinwords:
724 Unlocking hyper-detailed image descriptions. *arXiv preprint arXiv:2405.02793*, 2024. 24
- 725 Yash Goyal, Tejas Khot, Douglas Summers-Stay, Dhruv Batra, and Devi Parikh. Making the v in vqa
726 matter: Elevating the role of image understanding in visual question answering. In *Proceedings of
727 the IEEE conference on computer vision and pattern recognition*, pp. 6904–6913, 2017. 32, 34, 37
- 728 Kristen Grauman, Andrew Westbury, Eugene Byrne, Zachary Chavis, Antonino Furnari, Rohit
729 Girdhar, Jackson Hamburger, Hao Jiang, Miao Liu, Xingyu Liu, et al. Ego4D: Around the world
730 in 3,000 hours of egocentric video. In *Proceedings of the IEEE/CVF Conference on Computer
731 Vision and Pattern Recognition*, pp. 18995–19012, 2022. 1, 5, 6, 26
- 732 Kristen Grauman, Andrew Westbury, Lorenzo Torresani, Kris Kitani, Jitendra Malik, Triantafyllos
733 Afouras, Kumar Ashutosh, Vijay Baiyya, Siddhant Bansal, Bikram Boote, et al. Ego-exo4d:
734 Understanding skilled human activity from first-and third-person perspectives. *arXiv preprint
735 arXiv:2311.18259*, 2023. 1, 2
- 736 Mingfei Han, Xiaojun Chang, Heng Wang, and Linjie Yang. Shot2story20k: A new benchmark for
737 comprehensive understanding of multi-shot videos. *arXiv preprint arXiv:2312.10300*, 2023. 24
- 738 Jinyi Hu, Yuan Yao, Chongyi Wang, Shan Wang, Yinxu Pan, Qianyu Chen, Tianyu Yu, Hanghao Wu,
739 Yue Zhao, Haoye Zhang, Xu Han, Yankai Lin, Jiao Xue, Dahai Li, Zhiyuan Liu, and Maosong Sun.
740 Large multilingual models pivot zero-shot multimodal learning across languages. *arXiv preprint
741 arXiv:2308.12038*, 2023. 4
- 742 Ting-Hao Huang, Francis Ferraro, Nasrin Mostafazadeh, Ishan Misra, Aishwarya Agrawal, Jacob
743 Devlin, Ross Girshick, Xiaodong He, Pushmeet Kohli, Dhruv Batra, et al. Visual storytelling.
744 In *Proceedings of the 2016 conference of the North American chapter of the association for
745 computational linguistics: Human language technologies*, pp. 1233–1239, 2016. 34
- 746 Drew A Hudson and Christopher D Manning. GQA: A new dataset for real-world visual reasoning
747 and compositional question answering. In *Proceedings of the IEEE/CVF conference on computer
748 vision and pattern recognition*, pp. 6700–6709, 2019. 29, 32, 37
- 749 Minyoung Huh, Brian Cheung, Tongzhou Wang, and Phillip Isola. The platonic representation
750 hypothesis. *arXiv preprint arXiv:2405.07987*, 2024. 4

- 756 Vladimir Iashin and Esa Rahtu. A better use of audio-visual cues: Dense video captioning with
757 bi-modal transformer. *arXiv preprint arXiv:2005.08271*, 2020. 23
758
- 759 Jitesh Jain, Jianwei Yang, and Humphrey Shi. Vcoder: Versatile vision encoders for multimodal
760 large language models. *arXiv preprint arXiv:2312.14233*, 2023. 34
761
- 762 Peng Jin, Ryuichi Takanobu, Wancai Zhang, Xiaochun Cao, and Li Yuan. Chat-univi: Unified
763 visual representation empowers large language models with image and video understanding. In
764 *Proceedings of the IEEE/CVF Conference on Computer Vision and Pattern Recognition*, pp.
765 13700–13710, 2024. 23, 24
- 766 Justin Johnson, Bharath Hariharan, Laurens Van Der Maaten, Li Fei-Fei, C Lawrence Zitnick, and
767 Ross Girshick. Clevr: A diagnostic dataset for compositional language and elementary visual
768 reasoning. In *Proceedings of the IEEE conference on computer vision and pattern recognition*, pp.
769 2901–2910, 2017. 34
770
- 771 Xuan Ju, Yiming Gao, Zhaoyang Zhang, Ziyang Yuan, Xintao Wang, Ailing Zeng, Yu Xiong, Qiang
772 Xu, and Ying Shan. Miradata: A large-scale video dataset with long durations and structured
773 captions. *arXiv preprint arXiv:2407.06358*, 2024. 2, 6, 34, 39
- 774 Siddharth Karamcheti, Suraj Nair, Ashwin Balakrishna, Percy Liang, Thomas Kollar, and Dorsa
775 Sadigh. Prismatic vlms: Investigating the design space of visually-conditioned language models.
776 *arXiv preprint arXiv:2402.07865*, 2024. 3
777
- 778 Maxime Kayser, Oana-Maria Camburu, Leonard Salewski, Cornelius Emde, Virginie Do, Zeynep
779 Akata, and Thomas Lukasiewicz. e-vil: A dataset and benchmark for natural language explanations
780 in vision-language tasks. In *Proceedings of the IEEE/CVF international conference on computer
781 vision*, pp. 1244–1254, 2021. 34
- 782 Alexander Kirillov, Eric Mintun, Nikhila Ravi, Hanzi Mao, Chloe Rolland, Laura Gustafson, Tete
783 Xiao, Spencer Whitehead, Alexander C Berg, Wan-Yen Lo, et al. Segment anything. In *Proceedings
784 of the IEEE/CVF International Conference on Computer Vision*, pp. 4015–4026, 2023. 27
785
- 786 Jonathan Krause, Justin Johnson, Ranjay Krishna, and Li Fei-Fei. A hierarchical approach for
787 generating descriptive image paragraphs. In *Proceedings of the IEEE conference on computer
788 vision and pattern recognition*, pp. 317–325, 2017. 34
- 789 Ranjay Krishna, Kenji Hata, Frederic Ren, Li Fei-Fei, and Juan Carlos Niebles. Dense-captioning
790 events in videos. In *Proceedings of the IEEE international conference on computer vision*, pp.
791 706–715, 2017a. 2
792
- 793 Ranjay Krishna, Yuke Zhu, Oliver Groth, Justin Johnson, Kenji Hata, Joshua Kravitz, Stephanie
794 Chen, Yannis Kalantidis, Li-Jia Li, David A Shamma, et al. Visual genome: Connecting language
795 and vision using crowdsourced dense image annotations. *International journal of computer vision*,
796 123:32–73, 2017b. 27
- 797 Hugo Laurençon, Léo Tronchon, Matthieu Cord, and Victor Sanh. What matters when building
798 vision-language models? *arXiv preprint arXiv:2405.02246*, 2024. 3
799
- 800 Paul Lerner, Olivier Ferret, Camille Guinaudeau, Hervé Le Borgne, Romaric Besançon, José G
801 Moreno, and Jesús Lovón Melgarejo. Viquae, a dataset for knowledge-based visual question
802 answering about named entities. In *Proceedings of the 45th International ACM SIGIR Conference
803 on Research and Development in Information Retrieval*, pp. 3108–3120, 2022. 34
- 804 Bo Li, Yuanhan Zhang, Dong Guo, Renrui Zhang, Feng Li, Hao Zhang, Kaichen Zhang, Yanwei
805 Li, Ziwei Liu, and Chunyuan Li. LLaVA-OneVision: Easy visual task transfer. *arXiv preprint
806 arXiv:2408.03326*, 2024a. 3, 8, 9, 34
807
- 808 Boyi Li, Ligeng Zhu, Ran Tian, Shuhan Tan, Yuxiao Chen, Yao Lu, Yin Cui, Sushant Veer, Max
809 Ehrlich, Jonah Philion, et al. Wolf: Captioning everything with a world summarization framework.
arXiv preprint arXiv:2407.18908, 2024b. 2, 5

- 810 Junnan Li, Dongxu Li, Silvio Savarese, and Steven Hoi. Blip-2: Bootstrapping language-image
811 pre-training with frozen image encoders and large language models. In *International conference*
812 *on machine learning*, pp. 19730–19742. PMLR, 2023a. 1
- 813 Junyan Li, Delin Chen, Tianle Cai, Peihao Chen, Yining Hong, Zhenfang Chen, Yikang Shen, and
814 Chuang Gan. Flexattention for efficient high-resolution vision-language models. *arXiv preprint*
815 *arXiv:2407.20228*, 2024c. 23
- 816 KunChang Li, Yanan He, Yi Wang, Yizhuo Li, Wenhai Wang, Ping Luo, Yali Wang, Limin Wang,
817 and Yu Qiao. Videochat: Chat-centric video understanding. *arXiv preprint arXiv:2305.06355*,
818 2023b. 5, 7, 8, 9, 23
- 819 Lei Li, Yuwei Yin, Shicheng Li, Liang Chen, Peiyi Wang, Shuhuai Ren, Mukai Li, Yazheng
820 Yang, Jingjing Xu, Xu Sun, et al. M3IT: A large-scale dataset towards multi-modal multilingual
821 instruction tuning. *arXiv preprint arXiv:2306.04387*, 2023c. 34
- 822 Qingyun Li, Zhe Chen, Weiyun Wang, Wenhai Wang, Shenglong Ye, Zhenjiang Jin, Guanzhou Chen,
823 Yanan He, Zhangwei Gao, Erfei Cui, et al. Omnicorpus: An unified multimodal corpus of 10
824 billion-level images interleaved with text. *arXiv preprint arXiv:2406.08418*, 2024d. 24
- 825 Wei Li, Linchao Zhu, Longyin Wen, and Yi Yang. Decap: Decoding clip latents for zero-shot
826 captioning via text-only training. *arXiv preprint arXiv:2303.03032*, 2023d. 4, 5
- 827 Xiaotong Li, Fan Zhang, Haiwen Diao, Yueze Wang, Xinlong Wang, and Ling-Yu Duan.
828 Densefusion-1m: Merging vision experts for comprehensive multimodal perception. *arXiv preprint*
829 *arXiv:2407.08303*, 2024e. 34
- 830 Xirong Li, Weiyu Lan, Jianfeng Dong, and Hailong Liu. Adding chinese captions to images. In
831 *Proceedings of the 2016 ACM on international conference on multimedia retrieval*, pp. 271–275,
832 2016. 34
- 833 Xirong Li, Chaoxi Xu, Xiaoxu Wang, Weiyu Lan, Zhengxiong Jia, Gang Yang, and Jieping Xu. Coco-
834 cn for cross-lingual image tagging, captioning, and retrieval. *IEEE Transactions on Multimedia*,
835 21(9):2347–2360, 2019. 34
- 836 Xirui Li, Chao Ma, Xiaokang Yang, and Ming-Hsuan Yang. Vidtome: Video token merging for
837 zero-shot video editing. *arXiv preprint arXiv:2312.10656*, 2023e. 2
- 838 Yanwei Li, Chengyao Wang, and Jiaya Jia. Llama-vid: An image is worth 2 tokens in large language
839 models. *arXiv preprint arXiv:2311.17043*, 2023f. 2, 8, 9, 23
- 840 Yanwei Li, Chengyao Wang, and Jiaya Jia. Llama-vid: An image is worth 2 tokens in large language
841 models. *arXiv preprint arXiv:2311.17043*, 2023g. 2, 5
- 842 Yifan Li, Yifan Du, Kun Zhou, Jinpeng Wang, Wayne Xin Zhao, and Ji-Rong Wen. Evaluating object
843 hallucination in large vision-language models. *arXiv preprint arXiv:2305.10355*, 2023h. 37
- 844 Bin Lin, Bin Zhu, Yang Ye, Munan Ning, Peng Jin, and Li Yuan. Video-llava: Learning united visual
845 representation by alignment before projection. *arXiv preprint arXiv:2311.10122*, 2023a. 5, 8, 9, 23
- 846 Chin-Yew Lin. Rouge: A package for automatic evaluation of summaries. In *Text summarization*
847 *branches out*, pp. 74–81, 2004. 7, 9, 10, 23
- 848 Ji Lin, Hongxu Yin, Wei Ping, Yao Lu, Pavlo Molchanov, Andrew Tao, Huizi Mao, Jan Kautz,
849 Mohammad Shoeybi, and Song Han. Vila: On pre-training for visual language models. *arXiv*
850 *preprint arXiv:2312.07533*, 2023b. 8, 9, 23
- 851 Tsung-Yi Lin, Michael Maire, Serge Belongie, James Hays, Pietro Perona, Deva Ramanan, Piotr
852 Dollár, and C Lawrence Zitnick. Microsoft coco: Common objects in context. In *Computer Vision–*
853 *ECCV 2014: 13th European Conference, Zurich, Switzerland, September 6-12, 2014, Proceedings,*
854 *Part V 13*, pp. 740–755. Springer, 2014. 4, 27, 32, 34, 37
- 855 Feng Liu, Tao Xiang, Timothy M Hospedales, Wankou Yang, and Changyin Sun. ivqa: Inverse visual
856 question answering. In *Proceedings of the IEEE Conference on Computer Vision and Pattern*
857 *Recognition*, pp. 8611–8619, 2018. 33, 35

- 864 Haotian Liu, Chunyuan Li, Yuheng Li, and Yong Jae Lee. Improved baselines with visual instruction
865 tuning. *arXiv preprint arXiv:2310.03744*, 2023. 4, 8, 9, 34
866
- 867 Haotian Liu, Chunyuan Li, Yuheng Li, Bo Li, Yuanhan Zhang, Sheng Shen, and Yong Jae Lee.
868 Llava-next: Improved reasoning, ocr, and world knowledge, January 2024a. URL <https://llava-vl.github.io/blog/2024-01-30-llava-next/>. 4, 5, 8, 9, 10, 23, 34
869
- 870 Haotian Liu, Chunyuan Li, Qingyang Wu, and Yong Jae Lee. Visual instruction tuning. *Advances in*
871 *neural information processing systems*, 36, 2024b. 1, 5, 24, 34
872
- 873 Ilya Loshchilov and Frank Hutter. Decoupled weight decay regularization. *arXiv preprint*
874 *arXiv:1711.05101*, 2017. 37
- 875 Pan Lu, Swaroop Mishra, Tanglin Xia, Liang Qiu, Kai-Wei Chang, Song-Chun Zhu, Oyvind Tafjord,
876 Peter Clark, and Ashwin Kalyan. Learn to explain: Multimodal reasoning via thought chains for
877 science question answering. *Advances in Neural Information Processing Systems*, 35:2507–2521,
878 2022. 34
- 879 Fan Ma, Xiaojie Jin, Heng Wang, Yuchen Xian, Jiashi Feng, and Yi Yang. Vista-llama: Reliable
880 video narrator via equal distance to visual tokens. *arXiv preprint arXiv:2312.08870*, 2023. 23
881
- 882 Yunchuan Ma, Laiyun Qing, Guorong Li, Yuankai Qi, Quan Z Sheng, and Qingming Huang. Retrieval
883 enhanced zero-shot video captioning. *arXiv preprint arXiv:2405.07046*, 2024. 5
884
- 885 Muhammad Maaz, Hanoona Rasheed, Salman Khan, and Fahad Shahbaz Khan. Video-chatgpt:
886 Towards detailed video understanding via large vision and language models. *arXiv preprint*
887 *arXiv:2306.05424*, 2023. 2, 5, 8, 9, 23, 24, 45
- 888 Kartikeya Mangalam, Raiymbek Akshulakov, and Jitendra Malik. Egoschema: A diagnostic
889 benchmark for very long-form video language understanding. *Advances in Neural Information*
890 *Processing Systems*, 36:46212–46244, 2023. 24, 25
- 891 Kenneth Marino, Mohammad Rastegari, Ali Farhadi, and Roozbeh Mottaghi. Ok-vqa: A visual
892 question answering benchmark requiring external knowledge. In *Proceedings of the IEEE/cv*
893 *conference on computer vision and pattern recognition*, pp. 3195–3204, 2019. 34
894
- 895 Ahmed Masry, Do Xuan Long, Jia Qing Tan, Shafiq Joty, and Enamul Hoque. Chartqa: A bench-
896 mark for question answering about charts with visual and logical reasoning. *arXiv preprint*
897 *arXiv:2203.10244*, 2022. 37
- 898 Minesh Mathew, Dimosthenis Karatzas, and CV Jawahar. Docvqa: A dataset for vqa on document
899 images. In *Proceedings of the IEEE/CVF winter conference on applications of computer vision*,
900 pp. 2200–2209, 2021. 34, 37
- 901 Antoine Miech, Dimitri Zhukov, Jean-Baptiste Alayrac, Makarand Tapaswi, Ivan Laptev, and Josef
902 Sivic. Howto100m: Learning a text-video embedding by watching hundred million narrated
903 video clips. In *Proceedings of the IEEE/CVF international conference on computer vision*, pp.
904 2630–2640, 2019. 1
905
- 906 Anand Mishra, Shashank Shekhar, Ajeet Kumar Singh, and Anirban Chakraborty. Ocr-vqa: Visual
907 question answering by reading text in images. In *2019 international conference on document*
908 *analysis and recognition (ICDAR)*, pp. 947–952. IEEE, 2019. 27, 34
- 909 Mixkit. Free stock video clips, motion graphics, & music tracks, 2024. URL [https://mixkit.](https://mixkit.co/)
910 [co/](https://mixkit.co/). Accessed: 2024-08-24. 5, 6
911
- 912 Mathew Monfort, SouYoung Jin, Alexander Liu, David Harwath, Rogerio Feris, James Glass, and
913 Aude Oliva. Spoken moments: Learning joint audio-visual representations from video descriptions.
914 In *Proceedings of the IEEE/CVF Conference on Computer Vision and Pattern Recognition*, pp.
915 14871–14881, 2021. 2
- 916 Arsha Nagrani, Paul Hongsuck Seo, Bryan Seybold, Anja Hauth, Santiago Manen, Chen Sun, and
917 Cordelia Schmid. Learning audio-video modalities from image captions. In *European Conference*
on Computer Vision, pp. 407–426. Springer, 2022. 1

- 918 Maxime Oquab, Timothée Darcet, Théo Moutakanni, Huy V Vo, Marc Szafraniec, Vasil Khalidov,
919 Pierre Fernandez, Daniel HAZIZA, Francisco Massa, Alaaeldin El-Nouby, et al. Dinov2: Learning
920 robust visual features without supervision. *Transactions on Machine Learning Research*, 2023. 3
921
- 922 Kishore Papineni, Salim Roukos, Todd Ward, and Wei-Jing Zhu. Bleu: a method for automatic
923 evaluation of machine translation. In *Proceedings of the 40th annual meeting of the Association
924 for Computational Linguistics*, pp. 311–318, 2002. 2, 7, 8, 23
- 925 Pexels. Free images and video clips, 2024. URL <https://www.pexels.com/zh-cn/>.
926 Accessed: 2024-08-24. 5, 6
927
- 928 Pixabay. Stunning free images & royalty-free stock, 2024. URL <https://pixabay.com/>.
929 Accessed: 2024-08-24. 5, 6
- 930 Bryan A Plummer, Liwei Wang, Chris M Cervantes, Juan C Caicedo, Julia Hockenmaier, and
931 Svetlana Lazebnik. Flickr30k entities: Collecting region-to-phrase correspondences for richer
932 image-to-sentence models. In *Proceedings of the IEEE international conference on computer
933 vision*, pp. 2641–2649, 2015. 4, 37
934
- 935 Alec Radford, Jong Wook Kim, Chris Hallacy, Aditya Ramesh, Gabriel Goh, Sandhini Agarwal,
936 Girish Sastry, Amanda Askell, Pamela Mishkin, Jack Clark, et al. Learning transferable visual
937 models from natural language supervision. In *International conference on machine learning*, pp.
938 8748–8763. PMLR, 2021. 3
- 939 Ruchit Rawal, Khalid Saifullah, Ronen Basri, David Jacobs, Gowthami Somepalli, and Tom Goldstein.
940 Cinepile: A long video question answering dataset and benchmark. In *Synthetic Data for Computer
941 Vision Workshop@ CVPR 2024*, 2024. 24
942
- 943 Machel Reid, Nikolay Savinov, Denis Teplyashin, Dmitry Lepikhin, Timothy Lillicrap, Jean-baptiste
944 Alayrac, Radu Soricut, Angeliki Lazaridou, Orhan Firat, Julian Schrittwieser, et al. Gemini
945 1.5: Unlocking multimodal understanding across millions of tokens of context. *arXiv preprint
946 arXiv:2403.05530*, 2024. 8, 9
947
- 948 Shuhuai Ren, Sishuo Chen, Shicheng Li, Xu Sun, and Lu Hou. Testa: Temporal-spatial token
949 aggregation for long-form video-language understanding. *arXiv preprint arXiv:2310.19060*, 2023.
950 23
- 951 Marcus Rohrbach, Wei Qiu, Ivan Titov, Stefan Thater, Manfred Pinkal, and Bernt Schiele. Translating
952 video content to natural language descriptions. In *Proceedings of the IEEE international conference
953 on computer vision*, pp. 433–440, 2013. 2
954
- 955 Olga Russakovsky, Jia Deng, Hao Su, Jonathan Krause, Sanjeev Satheesh, Sean Ma, Zhiheng Huang,
956 Andrej Karpathy, Aditya Khosla, Michael Bernstein, et al. Imagenet large scale visual recognition
957 challenge. *International journal of computer vision*, 115:211–252, 2015. 34
- 958 Dustin Schwenk, Apoorv Khandelwal, Christopher Clark, Kenneth Marino, and Roozbeh Mottaghi.
959 A-okvqa: A benchmark for visual question answering using world knowledge. In *European
960 Conference on Computer Vision*, pp. 146–162. Springer, 2022. 34
961
- 962 Yuzhang Shang, Mu Cai, Bingxin Xu, Yong Jae Lee, and Yan Yan. Llava-prumerge: Adaptive token
963 reduction for efficient large multimodal models. *arXiv preprint arXiv:2403.15388*, 2024. 23
964
- 965 Oleksii Sidorov, Ronghang Hu, Marcus Rohrbach, and Amanpreet Singh. Textcaps: a dataset for
966 image captioning with reading comprehension. In *Computer Vision—ECCV 2020: 16th European
967 Conference, Glasgow, UK, August 23–28, 2020, Proceedings, Part II 16*, pp. 742–758. Springer,
968 2020. 34, 37
- 969 Gunnar A Sigurdsson, Gül Varol, Xiaolong Wang, Ali Farhadi, Ivan Laptev, and Abhinav Gupta.
970 Hollywood in homes: Crowdsourcing data collection for activity understanding. In *Computer
971 Vision—ECCV 2016: 14th European Conference, Amsterdam, The Netherlands, October 11–14,
2016, Proceedings, Part I 14*, pp. 510–526. Springer, 2016. 2

- 972 Amanpreet Singh, Vivek Natarajan, Meet Shah, Yu Jiang, Xinlei Chen, Dhruv Batra, Devi Parikh, and
973 Marcus Rohrbach. Towards vqa models that can read. In *Proceedings of the IEEE/CVF conference*
974 *on computer vision and pattern recognition*, pp. 8317–8326, 2019. 34
- 975
976 Enxin Song, Wenhao Chai, Guan hong Wang, Yucheng Zhang, Haoyang Zhou, Feiyang Wu, Xun
977 Guo, Tian Ye, Yan Lu, Jenq-Neng Hwang, et al. Moviechat: From dense token to sparse memory
978 for long video understanding. *arXiv preprint arXiv:2307.16449*, 2023. 2, 5, 8, 9, 23, 24
- 979 Enxin Song, Wenhao Chai, Tian Ye, Jenq-Neng Hwang, Xi Li, and Gaoang Wang. Moviechat+:
980 Question-aware sparse memory for long video question answering. *arXiv preprint*
981 *arXiv:2404.17176*, 2024. 2, 5, 23
- 982 Alane Suhr, Mike Lewis, James Yeh, and Yoav Artzi. A corpus of natural language for visual
983 reasoning. In *Proceedings of the 55th Annual Meeting of the Association for Computational*
984 *Linguistics (Volume 2: Short Papers)*, pp. 217–223, 2017. 34
- 985
986 Reuben Tan, Ximeng Sun, Ping Hu, Jui-hsien Wang, Hanieh Deilamsalehy, Bryan A Plummer,
987 Bryan Russell, and Kate Saenko. Koala: Key frame-conditioned long video-llm. *arXiv preprint*
988 *arXiv:2404.04346*, 2024. 23
- 989 Ryota Tanaka, Kyosuke Nishida, and Sen Yoshida. Visualmrc: Machine reading comprehension on
990 document images. In *Proceedings of the AAAI Conference on Artificial Intelligence*, volume 35,
991 pp. 13878–13888, 2021. 34
- 992 Chameleon Team. Chameleon: Mixed-modal early-fusion foundation models. *arXiv preprint*
993 *arXiv:2405.09818*, 2024. 4
- 994
995 Qwen team. Qwen2-vl. 2024. 23
- 996
997 Yoad Tewel, Yoav Shalev, Idan Schwartz, and Lior Wolf. Zerocap: Zero-shot image-to-text generation
998 for visual-semantic arithmetic. In *Proceedings of the IEEE/CVF Conference on Computer Vision*
999 *and Pattern Recognition*, pp. 17918–17928, 2022. 5
- 1000 Tristan Thrush, Ryan Jiang, Max Bartolo, Amanpreet Singh, Adina Williams, Douwe Kiela, and Can-
1001 dace Ross. Winoground: Probing vision and language models for visio-linguistic compositionality.
1002 In *Proceedings of the IEEE/CVF Conference on Computer Vision and Pattern Recognition*, pp.
1003 5238–5248, 2022. 34
- 1004 Yunjie Tian, Tianren Ma, Lingxi Xie, Jihao Qiu, Xi Tang, Yuan Zhang, Jianbin Jiao, Qi Tian,
1005 and Qixiang Ye. Chatterbox: Multi-round multimodal referring and grounding. *arXiv preprint*
1006 *arXiv:2401.13307*, 2024. 34
- 1007
1008 Shengbang Tong, Ellis Brown, Penghao Wu, Sanghyun Woo, Manoj Middepogu, Sai Charitha
1009 Akula, Jihan Yang, Shusheng Yang, Adithya Iyer, Xichen Pan, et al. Cambrian-1: A fully open,
1010 vision-centric exploration of multimodal llms. *arXiv preprint arXiv:2406.16860*, 2024a. 9, 34
- 1011 Shengbang Tong, Zhuang Liu, Yuexiang Zhai, Yi Ma, Yann LeCun, and Saining Xie. Eyes wide
1012 shut? exploring the visual shortcomings of multimodal llms. *arXiv preprint arXiv:2401.06209*,
1013 2024b. 4
- 1014
1015 Atousa Torabi, Christopher Pal, Hugo Larochelle, and Aaron Courville. Using descriptive video ser-
1016 vices to create a large data source for video annotation research. *arXiv preprint arXiv:1503.01070*,
1017 2015. 2
- 1018 Ramakrishna Vedantam, C Lawrence Zitnick, and Devi Parikh. Cider: Consensus-based image
1019 description evaluation. In *Proceedings of the IEEE conference on computer vision and pattern*
1020 *recognition*, pp. 4566–4575, 2015. 2, 7, 8, 23, 29
- 1021 Andreas Veit, Tomas Matera, Lukas Neumann, Jiri Matas, and Serge Belongie. Coco-text: Dataset and
1022 benchmark for text detection and recognition in natural images. *arXiv preprint arXiv:1601.07140*,
1023 2016. 29, 34
- 1024
1025 Han Wang, Yanjie Wang, Yongjie Ye, Yuxiang Nie, and Can Huang. Elysium: Exploring object-level
perception in videos via mllm. *arXiv preprint arXiv:2403.16558*, 2024a. 23

- 1026 Jianfeng Wang, Zhengyuan Yang, Xiaowei Hu, Linjie Li, Kevin Lin, Zhe Gan, Zicheng Liu, Ce Liu,
1027 and Lijuan Wang. Git: A generative image-to-text transformer for vision and language. *arXiv*
1028 *preprint arXiv:2205.14100*, 2022. 1
- 1029
- 1030 Jie Wang, Tao Ji, Yuanbin Wu, Hang Yan, Tao Gui, Qi Zhang, Xuanjing Huang, and Xiaoling
1031 Wang. Length generalization of causal transformers without position encoding. *arXiv preprint*
1032 *arXiv:2404.12224*, 2024b. 2
- 1033
- 1034 Junke Wang, Lingchen Meng, Zejia Weng, Bo He, Zuxuan Wu, and Yu-Gang Jiang. To see is to
1035 believe: Prompting gpt-4v for better visual instruction tuning. *arXiv preprint arXiv:2311.07574*,
2023. 34
- 1036
- 1037 Xin Wang, Jiawei Wu, Junkun Chen, Lei Li, Yuan-Fang Wang, and William Yang Wang. VateX: A
1038 large-scale, high-quality multilingual dataset for video-and-language research. In *Proceedings of*
1039 *the IEEE/CVF International Conference on Computer Vision*, pp. 4581–4591, 2019. 2, 4, 26, 29,
33, 35, 37, 42
- 1040
- 1041 Haoning Wu, Dongxu Li, Bei Chen, and Junnan Li. Longvideobench: A benchmark for long-context
1042 interleaved video-language understanding. *arXiv preprint arXiv:2407.15754*, 2024. 2
- 1043
- 1044 Penghao Wu and Saining Xie. V*: Guided visual search as a core mechanism in multimodal llms.
1045 *arXiv preprint arXiv:2312.14135*, 2023. 34
- 1046
- 1047 Wenhao Wu. Freeva: Offline mllm as training-free video assistant. *arXiv e-prints*, pp. arXiv–2405,
2024. 5, 23
- 1048
- 1049 Junbin Xiao, Xindi Shang, Angela Yao, and Tat-Seng Chua. Next-qa: Next phase of question-
1050 answering to explaining temporal actions. In *Proceedings of the IEEE/CVF conference on computer*
1051 *vision and pattern recognition*, pp. 9777–9786, 2021. 2
- 1052
- 1053 Dejing Xu, Zhou Zhao, Jun Xiao, Fei Wu, Hanwang Zhang, Xiangnan He, and Yueting Zhuang. Video
1054 question answering via gradually refined attention over appearance and motion. In *Proceedings of*
the 25th ACM international conference on Multimedia, pp. 1645–1653, 2017. 4, 33, 35, 37
- 1055
- 1056 Haiyang Xu, Qinghao Ye, Ming Yan, Yaya Shi, Jiabo Ye, Yuanhong Xu, Chenliang Li, Bin Bi,
1057 Qi Qian, Wei Wang, et al. mplug-2: A modularized multi-modal foundation model across text,
1058 image and video. In *International Conference on Machine Learning*, pp. 38728–38748. PMLR,
2023. 1
- 1059
- 1060 Jun Xu, Tao Mei, Ting Yao, and Yong Rui. Msr-vtt: A large video description dataset for bridging
1061 video and language. In *Proceedings of the IEEE conference on computer vision and pattern*
1062 *recognition*, pp. 5288–5296, 2016. 2, 4, 26, 29, 33, 35, 37, 42
- 1063
- 1064 Lin Xu, Yilin Zhao, Daquan Zhou, Zhijie Lin, See Kiong Ng, and Jiashi Feng. Pllava: Parameter-free
1065 llava extension from images to videos for video dense captioning. *arXiv preprint arXiv:2404.16994*,
2024a. 23
- 1066
- 1067 Mingze Xu, Mingfei Gao, Zhe Gan, Hong-You Chen, Zhengfeng Lai, Haiming Gang, Kai Kang, and
1068 Afshin Dehghan. Slowfast-llava: A strong training-free baseline for video large language models.
1069 *arXiv preprint arXiv:2407.15841*, 2024b. 29, 30
- 1070
- 1071 Hongwei Xue, Tiankai Hang, Yanhong Zeng, Yuchong Sun, Bei Liu, Huan Yang, Jianlong Fu, and
1072 Baining Guo. Advancing high-resolution video-language representation with large-scale video
1073 transcriptions. In *Proceedings of the IEEE/CVF Conference on Computer Vision and Pattern*
Recognition, pp. 5036–5045, 2022. 24
- 1074
- 1075 Shen Yan, Tao Zhu, Zirui Wang, Yuan Cao, Mi Zhang, Soham Ghosh, Yonghui Wu, and Jiahui Yu.
1076 Videococa: Video-text modeling with zero-shot transfer from contrastive captioners. *arXiv preprint*
1077 *arXiv:2212.04979*, 2022. 1
- 1078
- 1079 Antoine Yang, Antoine Miech, Josef Sivic, Ivan Laptev, and Cordelia Schmid. Just ask: Learning to
answer questions from millions of narrated videos. In *Proceedings of the IEEE/CVF international*
conference on computer vision, pp. 1686–1697, 2021. 4, 5, 37

- 1080 Antoine Yang, Antoine Miech, Josef Sivic, Ivan Laptev, and Cordelia Schmid. Zero-shot video
1081 question answering via frozen bidirectional language models. *Advances in Neural Information*
1082 *Processing Systems*, 35:124–141, 2022. 5
- 1083
1084 Antoine Yang, Arsha Nagrani, Paul Hongsuck Seo, Antoine Miech, Jordi Pont-Tuset, Ivan Laptev,
1085 Josef Sivic, and Cordelia Schmid. Vid2seq: Large-scale pretraining of a visual language model for
1086 dense video captioning. In *Proceedings of the IEEE/CVF Conference on Computer Vision and*
1087 *Pattern Recognition*, pp. 10714–10726, 2023a. 1, 23
- 1088 Mengjiao Yang, Yilun Du, Kamyar Ghasemipour, Jonathan Tompson, Dale Schuurmans, and Pieter
1089 Abbeel. Learning interactive real-world simulators. *arXiv preprint arXiv:2310.06114*, 2023b. 1
- 1090
1091 Barry Menglong Yao, Aditya Shah, Lichao Sun, Jin-Hee Cho, and Lifu Huang. End-to-end multi-
1092 modal fact-checking and explanation generation: A challenging dataset and models. In *Proceedings*
1093 *of the 46th International ACM SIGIR Conference on Research and Development in Information*
1094 *Retrieval*, pp. 2733–2743, 2023. 34
- 1095 Hanrong Ye, Haotian Zhang, Erik Daxberger, Lin Chen, Zongyu Lin, Yanghao Li, Bowen Zhang,
1096 Haoxuan You, Dan Xu, Zhe Gan, et al. Mm-ego: Towards building egocentric multimodal llms.
1097 *arXiv preprint arXiv:2410.07177*, 2024. 24
- 1098
1099 Peter Young, Alice Lai, Micah Hodosh, and Julia Hockenmaier. From image descriptions to visual
1100 denotations: New similarity metrics for semantic inference over event descriptions. *Transactions*
1101 *of the Association for Computational Linguistics*, 2:67–78, 2014. 32
- 1102
1103 Zhou Yu, Dejing Xu, Jun Yu, Ting Yu, Zhou Zhao, Yueting Zhuang, and Dacheng Tao. Activitynet-qa:
1104 A dataset for understanding complex web videos via question answering. In *Proceedings of the*
1105 *AAAI Conference on Artificial Intelligence*, volume 33, pp. 9127–9134, 2019. 4, 29, 33, 35, 37
- 1106 Xiang Yue, Yuansheng Ni, Kai Zhang, Tianyu Zheng, Ruoqi Liu, Ge Zhang, Samuel Stevens,
1107 Dongfu Jiang, Weiming Ren, Yuxuan Sun, et al. Mmmu: A massive multi-discipline multimodal
1108 understanding and reasoning benchmark for expert agi. *arXiv preprint arXiv:2311.16502*, 2023.
1109 32, 37
- 1110
1111 Rowan Zellers, Yonatan Bisk, Ali Farhadi, and Yejin Choi. From recognition to cognition: Visual
1112 commonsense reasoning. In *Proceedings of the IEEE/CVF conference on computer vision and*
1113 *pattern recognition*, pp. 6720–6731, 2019. 34
- 1114 Hang Zhang, Xin Li, and Lidong Bing. Video-llama: An instruction-tuned audio-visual language
1115 model for video understanding. *arXiv preprint arXiv:2306.02858*, 2023a. 5, 23
- 1116
1117 Pan Zhang, Xiaoyi Dong, Yuhang Zang, Yuhang Cao, Rui Qian, Lin Chen, Qipeng Guo, Haodong
1118 Duan, Bin Wang, Linke Ouyang, et al. Internlm-xcomposer-2.5: A versatile large vision language
1119 model supporting long-contextual input and output. *arXiv preprint arXiv:2407.03320*, 2024a. 23
- 1120 Peiyuan Zhang, Kaichen Zhang, Bo Li, Guangtao Zeng, Jingkang Yang, Yuanhan Zhang, Ziyue
1121 Wang, Haoran Tan, Chunyuan Li, and Ziwei Liu. Long context transfer from language to vision.
1122 *arXiv preprint arXiv:2406.16852*, 2024b. URL <https://arxiv.org/abs/2406.16852>.
1123 8, 9
- 1124
1125 Renrui Zhang, Jiaming Han, Chris Liu, Peng Gao, Aojun Zhou, Xiangfei Hu, Shilin Yan, Pan Lu,
1126 Hongsheng Li, and Yu Qiao. Llama-adapter: Efficient fine-tuning of language models with zero-init
1127 attention. *arXiv preprint arXiv:2303.16199*, 2023b. 23
- 1128
1129 Ruohong Zhang, Liangke Gui, Zhiqing Sun, Yihao Feng, Keyang Xu, Yuanhan Zhang, Di Fu,
1130 Chunyuan Li, Alexander Hauptmann, Yonatan Bisk, et al. Direct preference optimization of video
1131 large multimodal models from language model reward. *arXiv preprint arXiv:2404.01258*, 2024c.
1132 23, 24, 34
- 1133 Tianyi Zhang, Varsha Kishore, Felix Wu, Kilian Q Weinberger, and Yoav Artzi. Bertscore: Evaluating
text generation with bert. In *International Conference on Learning Representations*, 2019. 23

- 1134 Yuanhan Zhang, Bo Li, haotian Liu, Yong jae Lee, Liangke Gui, Di Fu, Jiashi Feng, Ziwei Liu, and
1135 Chunyuan Li. Llava-next: A strong zero-shot video understanding model, April 2024d. URL
1136 <https://llava-vl.github.io/blog/2024-04-30-llava-next-video/>. 8, 9
1137
- 1138 Yue Zhao, Long Zhao, Xingyi Zhou, Jialin Wu, Chun-Te Chu, Hui Miao, Florian Schroff, Hartwig
1139 Adam, Ting Liu, Boqing Gong, et al. Distilling vision-language models on millions of videos.
1140 *arXiv preprint arXiv:2401.06129*, 2024a. 23
- 1141 Zhonghan Zhao, Wenhao Chai, Xuan Wang, Li Boyi, Shengyu Hao, Shidong Cao, Tian Ye, Jenq-
1142 Neng Hwang, and Gaoang Wang. See and think: Embodied agent in virtual environment. *arXiv*
1143 *preprint arXiv:2311.15209*, 2023. 1
- 1144 Zhonghan Zhao, Wenhao Chai, Xuan Wang, Ke Ma, Kewei Chen, Dongxu Guo, Tian Ye, Yanting
1145 Zhang, Hongwei Wang, and Gaoang Wang. Steve series: Step-by-step construction of agent
1146 systems in minecraft. *Computer Vision and Pattern Recognition Workshop*, 2024b. 1
1147
- 1148 Zhonghan Zhao, Kewei Chen, Dongxu Guo, Wenhao Chai, Tian Ye, Yanting Zhang, and Gaoang
1149 Wang. Hierarchical auto-organizing system for open-ended multi-agent navigation. *arXiv preprint*
1150 *arXiv:2403.08282*, 2024c. 1
- 1151 Zhonghan Zhao, Ke Ma, Wenhao Chai, Xuan Wang, Kewei Chen, Dongxu Guo, Yanting Zhang,
1152 Hongwei Wang, and Gaoang Wang. Do we really need a complex agent system? distill embodied
1153 agent into a single model. *arXiv preprint arXiv:2404.04619*, 2024d. 1
1154
- 1155 Yinhe Zheng, Guanyi Chen, Xin Liu, and Jian Sun. Mmchat: Multi-modal chat dataset on social
1156 media. *arXiv preprint arXiv:2108.07154*, 2021. 34
- 1157 Luowei Zhou, Chenliang Xu, and Jason Corso. Towards automatic learning of procedures from web
1158 instructional videos. In *Proceedings of the AAAI Conference on Artificial Intelligence*, volume 32,
1159 2018. 2, 23
1160
- 1161 Xingyi Zhou, Anurag Arnab, Shyamal Buch, Shen Yan, Austin Myers, Xuehan Xiong, Arsha Nagrani,
1162 and Cordelia Schmid. Streaming dense video captioning. *arXiv preprint arXiv:2404.01297*, 2024.
1163 23
1164
1165
1166
1167
1168
1169
1170
1171
1172
1173
1174
1175
1176
1177
1178
1179
1180
1181
1182
1183
1184
1185
1186
1187

Supplementary Material

The supplementary material is structured as follows:

- literature review about the related works in Section A.
- [More results on long video benchmarks in Section B.](#)
- [N-gram based evaluation metrics in Section C.](#)
- Benchmark comparison between VDC and other video captioning benchmarks in Section D.
- The calculation and the visualization examples of token merging in Section E.
- More ablation studies for AURORACAP in Section F.
- The training settings for AURORACAP in Section G.
- The introduction of the used evaluation benchmarks and settings in Section H.
- More limitations of AURORACAP at current stage in Section I.
- [Additional evaluation metrics analysis in Section J.](#)
- Prompt template of VDC generation in Section K.
- Question-answer pairs generation prompt template of VDCSCORE in Section L.
- More statistics information of VDC in Section M.
- More statistics information of VDCSCORE in Section N.
- Calculation details of Elo ranking in Section O.
- Case studies among several baselines in Section P.
- [Prompt template of predicted answers extraction in Section Q.](#)
- [Prompt template of correctness evaluation in Section R.](#)

A RELATED WORKS

Video Captioning The general goal of video captioning is understanding a video and describing it with natural language. Unlike image captioning, video captioning requires the description also on the temporal dimension (*e.g.*, human action, camera and object movement). The current datasets including videos in the domain of human activities (Caba Heilbron et al., 2015), cooking scene (Zhou et al., 2018; Iashin & Rahtu, 2020), movie (Song et al., 2023), and open domain (Chen & Dolan, 2011). In Table 1, we show the summary of current video captioning benchmarks. Most of them are with short caption, which is not suitable for evaluating video detailed captioning task. There are several widely used metrics to evaluate the correctness of generated caption, such as BLEU (Papineni et al., 2002), ROUGE-L (Lin, 2004), CIDEr (Vedantam et al., 2015), SPICE (Anderson et al., 2016), and BERTScore (Zhang et al., 2019). Dense Video Captioning (Yang et al., 2023a; Zhou et al., 2024) is also a captioning task but further requires localizing the events temporally. In this paper, we focus on the detailed description of a short video clip, where there are no scene changes or camera switches.

Large Multimodal Models for Video With the develop of LLMs and LMMs (Maaz et al., 2023; Zhang et al., 2023b; Li et al., 2023f; Song et al., 2023; Zhang et al., 2023a; Song et al., 2024; Zhao et al., 2024a; Zhou et al., 2024; team, 2024; Jin et al., 2024; Beyer et al., 2024; Shang et al., 2024; Cai et al., 2024; Cheng et al., 2024; Li et al., 2024c), many recent works have explored adapting them into video understanding field (*e.g.*, Video-LLaMA (Li et al., 2023f), Video-LLaVA (Lin et al., 2023a), VideoChat (Li et al., 2023b), Vista-LLaMA (Ma et al., 2023), LLaVA-Hound (Zhang et al., 2024c), Koala (Tan et al., 2024), Elysium (Wang et al., 2024a), and MovieChat (Song et al., 2023; 2024)). Thanks to this flexible design, the models can combine pretrained knowledge with minimal trainable parameters. Instead of requiring large-scale training, using only a small amount of high-quality training data can even achieve better results. Most of the existing models use additional parameters for temporal modeling. There are also some interesting observations that we can actually build advancing LMMs without additional parameters for temporal modeling (Xu et al., 2024a; Lin et al., 2023b; Liu et al., 2024a; Zhang et al., 2024a; Ren et al., 2023) or even without further training with video-text data (Wu, 2024). Recent works (*e.g.*, FreeVA (Wu, 2024), LLaVA-Next (Liu et al., 2024a), VLIA (Lin et al., 2023b), and PLLaVA (Xu et al., 2024a)) also find that the vanilla LLaVA-like model pretrained on high-quality image instruction data can also be a strong video understanding model. FreeVA further observe that using existing video instruction tuning data like Video-ChatGPT 100K (Maaz et al., 2023) to tune LMMs may not necessarily lead to improvements. As the concurrent work, we

also observe this phenomenon and proceeded to develop a video detailed captioning baseline training based on the LLaVA architecture. Chat-UniVi (Jin et al., 2024) employ a set of dynamic visual tokens to uniformly represent images and videos. However, for current video inputs, when we sample at 1 FPS, the frames are already sufficiently sparse; frame-to-frame similarity is quite low except in static scenes. On the other hand, if we use keyframes as input, the frame similarity will be even lower. Under these conditions, we believe that strong temporal merging should be avoided, as it is likely to impair the model’s core capabilities, especially since the CLIP vision encoder trained on images.

As for the benchmark, inspired by LLaVA (Liu et al., 2024b), Video-ChatGPT (Maaz et al., 2023) introduces a 100K video clips with text instructions with the first vLMMs benchmark evaluation system powered by LLMs. MovieChat-1K (Song et al., 2023) and CinePile (Rawal et al., 2024) are question-answering based benchmark for long-form video understanding. Shot2Story20K (Han et al., 2023) comprises videos with 2 to 8 shots each sourced for our dataset from the public video benchmark HDvila100M (Xue et al., 2022). However, currently there is no video benchmark available to evaluate video detailed captioning tasks like IIW (Garg et al., 2024) and other datasets (Li et al., 2024d) did in image captioning field. Other works (Ye et al., 2024) focus on the specific domain like Ego. In this paper, our work fills this gap. As for metric, LLaVA-Hound-DPO (Zhang et al., 2024c) uses similar divide-and-conquer strategy to build a preference dataset, ensuring that instructional data remains factually consistent with detailed captions. Our goal for VDCSCORE, however, is to evaluate the accuracy of generated captions through QA pairs generated from ground truth.

B MORE RESULTS ON LONG-FORM VIDEO BENCHMARKS

We take MovieChat-1K (Song et al., 2023), Egoschema (Mangalam et al., 2023) as the representative long video benchmark, and compare with existing models. As shown in the following Table B2 and Table B1, AURORACAP achieves comparable performance even without training on long videos and special design. We also plot the visual token kept ratio curve on EgoSchema as Figure B1, demonstrating the stability and effectiveness of our token merging method for longer video sequences.

Table B1: Model performance on Egoschema (Mangalam et al., 2023) benchmark.

Model	Design For Long Video	Accuracy
Random Choice	-	20.0
FrozenBiLM	×	26.9
mPLUG-Owl	×	31.1
TimeChat	✓	33.0
Video-LLAVA	×	38.4
LLAMA-VID	×	38.5
LLAVA-NeXT-Video	×	43.9
VideoLLAMA2	×	51.7
MovieChat	✓	53.5
Human Performance	-	76.2
AURORACAP (ours)	×	46.0

Table B2: Model performance on MovieChat-1K (Song et al., 2023) benchmark.

Model	Design for Long Video	Breakpoint	Global
Video-LLaMA	×	39.1	51.7
VideoChat	×	46.1	57.8
TimeChat	✓	46.1	73.8
VideoChatGPT	×	48.0	47.6
MovieChat	✓	48.3	62.3
MovieChat+	✓	49.6	71.2
AURORACAP (ours)	×	52.6	59.7

1296
1297
1298
1299
1300
1301
1302
1303
1304
1305
1306
1307
1308
1309
1310
1311
1312
1313
1314
1315
1316
1317
1318
1319
1320
1321
1322
1323
1324
1325
1326
1327
1328
1329
1330
1331
1332
1333
1334
1335
1336
1337
1338
1339
1340
1341
1342
1343
1344
1345
1346
1347
1348
1349

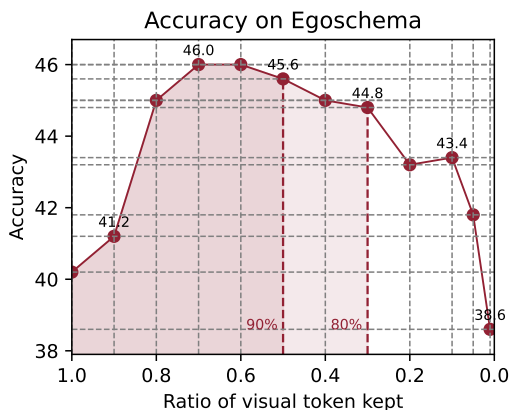


Figure B1: Token merging ablation curve on Egoschema (Mangalam et al., 2023). The best performance is set range from 0.6 to 0.7 of visual token kept ratio.

C N-GRAM BASED EVALUATION RESULTS

A variant of VDCSCORE could be developed to assess final triplets (<question, correct answer, predicted answer>) by employing a n-gram based evaluation approach as shown in Table C3 with correlation shown in Figure C2.

Table C3: Evaluation results of various models on VDC based on ROUGE for answer matching.

Model	Avg.	Camera	Short	Background	Main Object	Detailed
LLaMA-VID	6.66	9.53	5.12	5.30	6.07	7.29
Video-ChatGPT-7B	6.85	9.20	5.37	6.40	6.29	6.97
ViLA-7B	6.68	7.88	5.16	6.29	6.35	7.74
Video-LLAVA-7B	6.79	8.67	5.25	6.09	6.64	7.28
LLAVA-1.5-7B	6.34	8.31	5.40	5.80	5.52	6.65
LongVA-7B	6.70	8.37	4.99	6.11	6.79	7.23
LLAVA-1.5-13B	6.34	8.64	5.55	5.57	5.15	6.79
LLAVA-NeXT-V7B	6.69	8.61	5.30	6.35	6.27	6.93
LLAVA-1.6-7B	6.45	8.08	5.38	5.79	5.82	7.20
LLAVA-1.6-13B	6.18	7.31	5.28	6.00	5.29	7.01
ShareGPT4Video-8B	6.78	8.46	5.73	5.82	6.54	7.36
LLAVA-OV-7B	6.59	8.09	5.66	5.86	5.58	7.75
InternVL-2-8B	6.82	8.14	5.63	5.95	6.53	7.86
AURORACAP-7B	7.60	9.55	5.66	6.79	7.42	8.58
Gemini-1.5 Pro	7.59	8.78	6.25	7.29	7.70	7.94

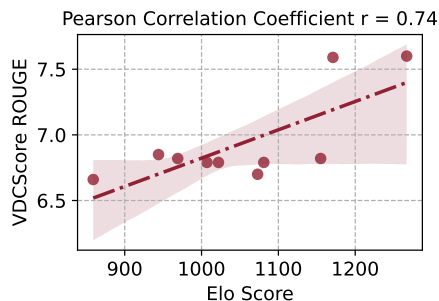


Figure C2: Correlation between the n-gram evaluation scores and human elo ranking on the VDC.

D BENCHMARK COMPARISON

We compare our proposed VDC with some examples from several video captioning benchmarks as shown in Figure D3, Figure D4, and Figure D5. The corresponding captions are shown as followings:



Figure D3: Video example of MSR-VTT (Xu et al., 2016) benchmark.

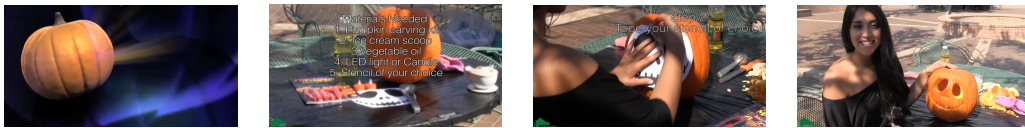


Figure D4: Video example of VATEX (Wang et al., 2019) benchmark.

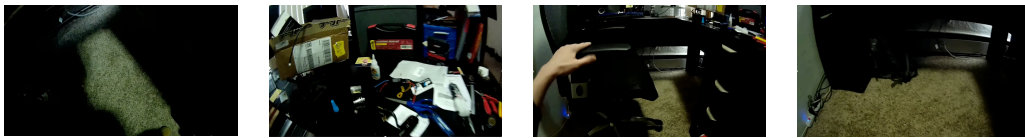


Figure D5: Video example of VDC benchmark sampled from Ego4D (Grauman et al., 2022).

Benchmark Caption (for VDC we show only the detailed caption)

MSR-VTT D3 (4 words) Teams are playing soccer.

VATEX D4 (13 words) A woman instructs and demonstrates how to remove the insides of a pumpkin.

VDC D5 (618 words) The video opens with an intimate close-up of a surface adorned with vibrant green moss and intricate lichen, initially evoking the serene beauty of a natural landscape. This organic imagery quickly transitions, revealing that the mossy surface is actually part of a motorcycle or vehicle's engine compartment, creating a striking contrast between the lush textures of nature and the cold, hard lines of mechanical components. As the camera angle shifts, the viewer is drawn deeper into the engine compartment, where the interplay of moss overgrowth on various machinery introduces a fascinating blend of organic life and industrial elements, highlighting the unexpected coexistence of nature and technology.

The perspective then zooms in, accentuating the rich details of the mossy growth, which clings tenaciously to the metallic surfaces, while a dark cavity beneath hints at the complexity of the machinery. The reflective metallic surfaces glint in the light, further enhancing the visual contrast and inviting the viewer to explore this unique juxtaposition. Suddenly, the scene shifts dramatically, with rapid camera motion creating a vibrant blur of colors and shapes, transforming the previously detailed views into a chaotic whirlwind, suggesting a swift movement through the intricate landscape of the engine compartment.

As the motion blur begins to dissipate, the viewer is presented with a clearer image of a light-colored, textured surface, where blurred mechanical components can be discerned, indicating a deceleration in movement. The camera stabilizes, revealing a rough-textured floor or ground that suggests an indoor or industrial environment, characterized by a sense of organized chaos. The scene transitions to a detailed examination of a cluttered workspace filled with tangled wires, casings, and components in a variety of colors, emphasizing the disorganized state of electronic or mechanical internals, possibly during a maintenance or repair process.

The perspective shifts once more, showcasing darker, textured surfaces juxtaposed against lighter insulating materials, with hidden metallic elements peeking through, suggesting another angle within this same cluttered interior space. A human hand enters the frame, reaching out to interact with the components, signaling an active workspace filled with purpose. As the scene expands, additional hands join the fray, actively manipulating various objects within the crowded environment, signifying an ongoing task or collaborative effort amidst the complex array of components and materials.

1404 The atmosphere is imbued with a sense of urgency and engagement, as the camera captures the
 1405 dynamic interactions of the individuals working together. The camera work remains fluid and
 1406 dynamic, featuring a mix of close-up shots that highlight the intricate details of the components
 1407 and wider angles that provide context to the bustling environment. The slightly shaky nature of
 1408 the shots adds a layer of realism and immersion, drawing the viewer into the heart of the action.
 1409 The low light conditions create a moody ambiance, with shadows dancing across the surfaces,
 1410 enhancing the visual depth and interest of the scene. Overall, the video encapsulates a vivid
 1411 portrayal of the intersection between nature and machinery, as well as the collaborative spirit of
 1412 those engaged in the intricate task of maintenance and repair within this unique setting.

1413 E TOKEN MERGING VISUALIZATION



1442 Figure E6: Token merging visualization. From top to bottom, the image IDs are COCO:COCO-
 1443 train2014-000000247906, VG:2331508, SA-1B:sa-393200, OCR-VQA:71789111. From left to right,
 1444 the number of tokens representing the images are 490, 154, 18, and 6.

1446 The number of tokens r merged in each layer of the transformer in ViT is calculated by the following
 1447 formula:

$$1448 \quad r = (1 - \text{ratio}) \cdot (W \cdot H / P^2) / L \quad (2)$$

1449 where W , H is the width and the height of the input image, P is the patch size, L is the number
 1450 of layers in the transformer, ratio is the proportion of tokens to be kept. The merging is evenly
 1451 distributed across all layers of the transformer.

1452 We show token merging visualization examples from COCO (Lin et al., 2014), VG (Krishna et al.,
 1453 2017b), SA-1B (Kirillov et al., 2023), and OCR-VQA (Mishra et al., 2019) in Figure E6, since we
 1454 only conduct frame-wise operation. Features extracted by CLIP ViT-H model². We conduct image
 1455 captioning for the examples given final token numbers by 7B AURORACAP as following. We remove
 1456 line breaks in generated caption for a better reading experience.

1457 ²Huggingface Model: <https://huggingface.co/apple/DFN5B-CLIP-ViT-H-14-378>

- 1458 **# Token Describe this image in detail. (Figure E6 Row 1)**
 1459
 1460 490 In the heart of a winter wonderland, a skier takes flight, suspended in mid-air against the backdrop
 1461 of a clear blue sky. The skier, clad in a vibrant red and white jacket, is captured in a moment of pure
 1462 exhilaration. The skier's body is angled towards the left side of the image, with their skis crossed in an
 1463 impressive display of skill and control. The skier's helmet, a stark contrast to the surrounding snow, is
 1464 adorned with a pink and white design, adding a touch of color to the otherwise monochrome landscape.
 1465 The skier's goggles, reflecting the bright sunlight, are a testament to the intensity of the sport. Beneath
 1466 the skier, the snow-covered mountain slopes stretch out, dotted with trees that stand as silent spectators
 1467 to the skier's daring feat. The image is a freeze-frame of action and adventure, encapsulating the thrill
 1468 and beauty of winter sports.
- 1468 154 In the midst of a clear blue sky, a skier is captured in a moment of thrilling action. The skier, clad in
 1469 a vibrant red and white jacket, is suspended in mid-air, performing an impressive trick. The skier's
 1470 body is parallel to the ground, creating a sense of motion and excitement. The skier's skis, a striking
 1471 combination of red and white, are crossed in front of them, adding to the dynamic nature of the image.
 1472 The skier's helmet, a necessary safety measure, is white and contrasts with the colorful jacket. The
 1473 backdrop to this action-packed scene is a breathtaking snowy mountain landscape. The mountain's
 1474 peak is visible in the distance, adding depth to the image. The overall composition of the image
 1475 suggests a high-speed descent down the mountain, with the skier skillfully navigating the terrain. This
 1476 image encapsulates the exhilarating sport of skiing, showcasing not only the skill of the skier but also
 1477 the stunning beauty of the mountain landscape.
- 1478 18 In the heart of a snowy mountain, a daring skier takes flight. Dressed in a vibrant red and white jacket,
 1479 black pants, and a protective white helmet, the skier is captured mid-air, performing an impressive
 1480 trick. The skier's body is parallel to the ground, arms outstretched, as if embracing the thrill of the
 1481 moment. The skier's skis, a striking combination of red and white, are pointed upwards towards
 1482 the clear blue sky. The skier's poles, held firmly in their hands, add to the dynamic nature of the
 1483 scene. The backdrop to this exhilarating moment is a breathtaking snowy mountain landscape. The
 1484 mountain's peak, blanketed in snow, stretches out into the distance. The clear blue sky above is devoid
 1485 of clouds, adding to the serene beauty of the scene. This image captures not just a moment, but a story
 1486 of adventure, thrill, and the sheer joy of skiing.
- 1487 6 The image captures a thrilling moment of a snowboarder in mid-air, performing an impressive trick.
 1488 The snowboarder, clad in a vibrant red and white jacket, black pants, and a protective helmet, is the
 1489 central figure in this dynamic scene. The snowboarder is holding onto a rope with one hand, suggesting
 1490 that they are being pulled up the mountain by a snowmobile, a common practice in snowboarding to
 1491 gain speed and momentum. The rope extends from the top left corner of the image, creating a sense
 1492 of movement and direction. The backdrop of the image is a breathtaking snowy mountain landscape,
 1493 complete with trees and other natural elements. The snowboarder is positioned in the center of the
 1494 image, drawing the viewer's attention to their daring stunt. The image is a testament to the exhilarating
 1495 sport of snowboarding and the skill and courage of the athletes who participate in it. It's a freeze-frame
 1496 of an adrenaline-fueled moment, encapsulating the thrill and excitement of snowboarding.
- 1497 **# Token What is the number in the picture? (Figure E6 Row 2)**
 1498
 1499 490 The number in the picture is "45". It is displayed on the back of the jersey that the person is wearing.
 1500 154 The number in the picture is "45".
 1501 18 The number in the picture is "45". It is displayed on the back of the baseball jersey worn by the player
 1502 in the image.
 1503 6 The number in the picture is "45". It is displayed in a large, bold font on the jersey of the baseball
 1504 player in the image.
- 1505 **# Token What is the relative position of the white and red cars in the picture? Which one in the**
 1506 **left? (Figure E6 Row 3)**
 1507
 1508 490 The white car is positioned to the left of the red car in the image. The white car is closer to the
 1509 foreground and is stopped at the traffic light, while the red car is further back, also stopped at the same
 1510 traffic light. The relative position of the cars is such that the white car is in the left lane and the red car
 1511 is in the right lane, both facing the same direction of traffic.
- 1505 154 The white car is positioned to the left of the red car in the image. The red car is further back on the
 1506 road, indicating it is behind the white car. This is determined by the perspective of the image, where
 1507 the white car is closer to the foreground and the red car is further away, both in the same lane and
 1508 moving in the same direction.
- 1509 18 The white car is on the left side of the image, and the red car is on the right side. The white car is
 1510 closer to the foreground, while the red car is further away, positioned behind the white car.
- 1511 6 The white car is on the left side of the image, while the red car is on the right side. The white car is
 positioned closer to the foreground, while the red car is further back, near the intersection.

F ABLATION STUDIES

In this section, we conduct the ablation studies in several aspects including token merging, slowfast inference, efficiency, training strategy, and backbone selection.

Token merging. As a core strategy of AURORACAP, token merging plays a significant role in reducing the number of visual tokens. We conduct extensive ablation studies to explore the impact of the token kept ratio $R_{v_{tk}}$ in terms of performance across multiple tasks including image captioning, visual question answering, video captioning, and video question answering as shown in Figure F9 and Figure F10. We define the performance percentage as the proportion between the highest and lowest values on the entire performance curve. We identify the minimum retention thresholds for achieving 90% and 80% performance. As shown in Figure F9, while the performance of AURORACAP generally declines with fewer visual tokens across most benchmarks, it remains relatively stable at higher retention levels. Most models maintain satisfactory performance ($> 80\%$) even with only 0.4 of $R_{v_{tk}}$, highlighting the efficiency of our approach. Visual token retention thresholds vary by task complexity, with more visually demanding tasks needing higher retention of visual tokens. For instance, CIDEr (Vedantam et al., 2015) on COCO-Cap (Veit et al., 2016) maintains over 90% performance with an $R_{v_{tk}}$ of 0.3, whereas accuracy on GQA (Hudson & Manning, 2019) drops to 90% when the $R_{v_{tk}}$ is reduced to 0.8. Unlike image understanding, the optimal performance across most video understanding benchmarks occurs at a relatively low $R_{v_{tk}}$ as depicted in Figure F10. And for MSR-VTT (Xu et al., 2016), VATEX (Wang et al., 2019), and ActivityNet-QA (Yu et al., 2019), even achieve better results at extremely low $R_{v_{tk}}$ (< 0.1). It indicates that comparing to image, video input have higher redundancy. Note that AURORACAP focuses on spatial visual token merging, while the temporal features introduce additional complexity to explore the token merging laws. Appendix E shows more calculation details and the visualization results of token merging.

Slowfast inference. Inspired by Slowfast-LLaVA (Xu et al., 2024b), we explore whether combining frames with low and high $R_{v_{tk}}$ can enhance performance. In practice, we don't conduct token merging in the first frame and concatenate them with the merged tokens from subsequent frames. We apply this strategy to both video captioning and video question answering tasks, comparing performance with and without the inclusion of full first-frame visual tokens. As illustrated in Table F4, slowfast inference brings marginal performance improvement in video question answering tasks or even drop in video captioning tasks but with more computing cost. Therefore, by default, we don't using slowfast inference for video detailed captioning.

We also present the performance curve with and without the inclusion of full first-frame visual tokens as the visual token kept ratio varies during inference across multiple video understanding tasks. As illustrated in Figure F11 and Figure F12, despite the inclusion of full first-frame visual tokens, slowfast inference does not consistently result in significantly positive effects on performance. In some cases, the incorporation of full first-frame visual tokens even worsens performance degradation as the kept ratio decreases, particularly in video captioning tasks.

Table F4: Ablation on slowfast inference for AURORACAP-7B. We present the average performance among different token merging ratio on various video understanding benchmarks. We show that slowfast inference brings marginal performance improvement in video question answering tasks or even drop in video captioning tasks but with more computing cost.

Setting	MSR-VTT					VATEX					ANet	MSVD	MSRVTT
	\bar{C}	$\bar{B@1}$	$\bar{B@4}$	\bar{M}	\bar{R}	\bar{C}	$\bar{B@1}$	$\bar{B@4}$	\bar{M}	\bar{R}	$\frac{Acc}{Acc}$	$\frac{Acc}{Acc}$	$\frac{Acc}{Acc}$
w/o slowfast	26.72	53.01	17.58	21.25	46.78	28.03	52.28	15.22	16.95	38.30	58.55	56.45	37.26
w/ slowfast	26.18	51.68	17.00	21.20	46.16	28.07	52.16	15.12	16.95	38.27	59.66	55.65	38.22
Δ	-0.54	-1.33	-0.58	-0.05	-0.62	+0.04	-0.12	-0.10	-0.01	-0.03	+1.11	-0.80	+0.96

Efficiency. To assess the inference speed, we utilize the inference time per video question-answering pair in seconds (TPV) as an evaluative metric. SGLang is an accelerated serving framework for LLMs and multimodal LLMs. We consider four settings including with or without token merging and SGLang. Figure F7 indicates the minimum TPV achievable in each settings across seven video understanding datasets. Reducing the visual tokens and using SGLang result in excellent inference times per video question-answering pair while all the datasets with short video and question inputs.

1566

1567

1568

1569

1570

1571

1572

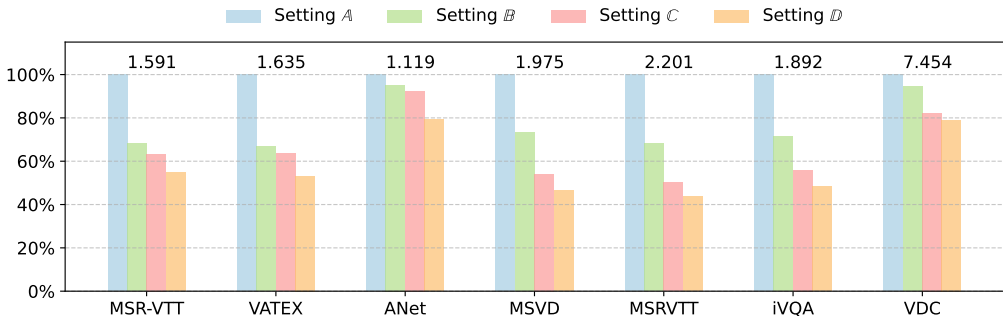
1573

1574

1575

1576

1577



1578

1579

1580

1581

1582

Figure F7: Comparison between different inference settings: \mathbb{A} : $R_{vtk} = 1.0$, without SGLang, \mathbb{B} : $R_{vtk} = 0.1$, without SGLang, \mathbb{C} : $R_{vtk} = 1.0$, with SGLang, \mathbb{D} : $R_{vtk} = 0.1$, with SGLang. The number indicates the maximum inference time in seconds for each benchmark.

1583

1584

1585

1586

In contrast, maintaining full visual tokens or omitting the use of SGLang results in comparatively slower performance, demonstrating the superior inference efficiency of AURORACAP. For each input, we process the video at a resolution of 378×378 and sample 8 frames using single H100 GPU.

1587

1588

1589

1590

Training strategy. Alternative training strategies for the language stage of AURORACAP are less frequently explored, which is the primary focus of this section. For a fair comparison, we use the same training datasets across all settings and maintain consistent hyper-parameters. The following training settings are explored:

1591

1592

1593

1594

1595

1596

1597

1598

1599

1600

1601

1602

1603

1604

1605

1606

1607

We implement these training strategies, track training costs in H100 hours, and evaluate across various video understanding tasks. As shown in Figure F8, while training with an R_{vtk} of 1.0 improves performance, it significantly increases training time. Surprisingly, mixing lower and higher visual token ratios during training offers no significant advantage. Training only the LLM under the two settings results in a performance drop, indicating that enhancing long video understanding still requires collaboration with the finetuning the visual encoder. Therefore, we choose Setting C as the final training strategy.

1608

1609

1610

Backbone selection. We use the the training loss among the last ten iterations in original LLaVA alignment pretraining stage to guidance the ViT and LLM backbones selection as shown in Table F5.

1611

1612

G DETAILED TRAINING SETTINGS

1613

1614

1615

1616

1617

1618

1619

We use CLIP ViT-H³, Vicuna-1.5-7B⁴ as the initialization of AURORACAP-7B. Training hyper-parameters for both stages are shown in Table G9. For visual data preprocessing, we resize each image or video frame to the short side of 378 while keeping original aspect. Instead of doing center crop, we conduct bilinear position embedding interpolation for each training sample. For video data, we extract frames at 2 FPS uniformly. For token merging, we use constant schedule for each blocks.

³Huggingface Model: <https://huggingface.co/apple/DFN5B-CLIP-ViT-H-14-378>

⁴Huggingface Model: <https://huggingface.co/lmsys/vicuna-7b-v1.5-16k>

1620
1621
1622
1623
1624
1625
1626
1627
1628
1629
1630
1631
1632
1633
1634
1635
1636
1637
1638
1639
1640
1641
1642
1643
1644
1645
1646
1647
1648
1649
1650
1651
1652
1653
1654
1655
1656
1657
1658
1659
1660
1661
1662
1663
1664
1665
1666
1667
1668
1669
1670
1671
1672
1673

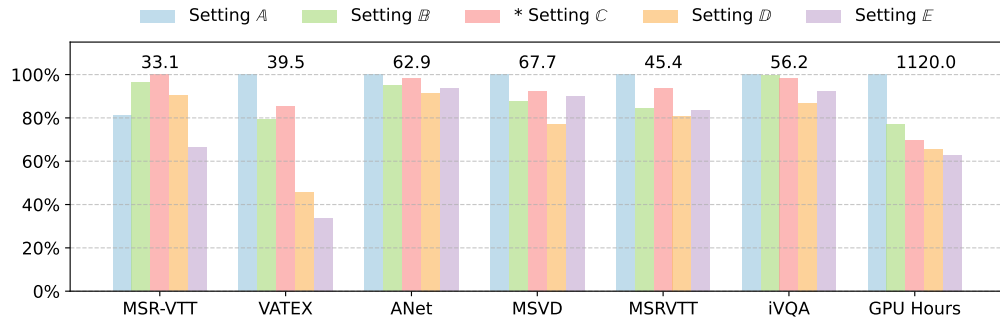


Figure F8: Comparison between different training strategy in Language stage. We take Accuracy for Question-Answering tasks and CIDEr for captioning tasks as the evaluation metric and present the performance percentage. We choose Setting C as the final training strategy as shown with *. The number shows the maximum value for each benchmark.

Table F5: Final training loss during pretraining stage with original LLaVA pretraining data.

ViT	ViT Size	LLM	LLM Size	Loss
facebook/dinov2-giant	1,136M	microsoft/phi-2	2.7B	3.3021
openai/clip-vit-large-patch14-336	428M	Qwen/Qwen1.5-0.5B-Chat	0.5B	3.1001
openai/clip-vit-large-patch14-336	428M	microsoft/phi-2	2.7B	2.8067
laion/CLIP-ViT-bigG-14-laion2B-39B-b160k	1,845M	microsoft/phi-2	2.7B	2.7124
facebook/dinov2-giant	1,136M	lmsys/vicuna-13b-v1.5	13B	2.3895
laion/CLIP-ViT-bigG-14-laion2B-39B-b160k	1,845M	internlm/internlm2-chat-7b	7B	2.3437
laion/CLIP-ViT-bigG-14-laion2B-39B-b160k	1,845M	internlm/internlm2-chat-20b	20B	2.2745
laion/CLIP-ViT-bigG-14-laion2B-39B-b160k	1,845M	deepseek-ai/deepseek-llm-67b-chat	67B	2.1572
laion/CLIP-ViT-bigG-14-laion2B-39B-b160k	1,845M	mistralai/Mistral-7B-Instruct-v0.1	7B	2.1569
openai/clip-vit-large-patch14-336	428M	mistralai/Mixtral-8x7B-Instruct-v0.1	8x7B	2.0815
apple/DFN5B-CLIP-ViT-H-14-378	632M	lmsys/vicuna-13b-v1.5-16k	13B	2.0443
laion/CLIP-ViT-bigG-14-laion2B-39B-b160k	1,845M	lmsys/vicuna-7b-v1.5-16k	7B	2.0365
laion/CLIP-ViT-bigG-14-laion2B-39B-b160k	1,845M	mistralai/Mixtral-8x7B-Instruct-v0.1	8x7B	1.9889
openai/clip-vit-large-patch14-336	428M	lmsys/vicuna-7b-v1.5	7B	1.9762
laion/CLIP-ViT-bigG-14-laion2B-39B-b160k	1,845M	meta-llama/Llama-2-13b-chat-hf	13B	1.9708
laion/CLIP-ViT-bigG-14-laion2B-39B-b160k	1,845M	lmsys/vicuna-13b-v1.5	13B	1.9412
apple/DFN5B-CLIP-ViT-H-14-378	632M	lmsys/vicuna-7b-v1.5-16k	7B	1.8679

H EVALUATION BENCHMARKS AND SETTINGS

We list all the hyper-parameters and prompt used for evaluation as shown in Table H10. For our proposed VDC, we show the settings as following with the max number of the tokens of 1,024:

Type Prompt used for evaluation

Camera Describe any camera zooms, pans, or angle changes.

Background Summarize the background setting of the video based on these frames.

Main Object Describe the main subject, including their attributes and movements throughout the video.

Detail Imagine the video from these frames and describe it in detail.

1674
1675
1676
1677
1678
1679
1680
1681
1682
1683
1684
1685
1686
1687
1688
1689
1690
1691
1692
1693
1694
1695
1696
1697
1698
1699
1700
1701
1702
1703
1704
1705
1706
1707
1708
1709
1710
1711
1712
1713
1714
1715
1716
1717
1718
1719
1720
1721
1722
1723
1724
1725
1726
1727

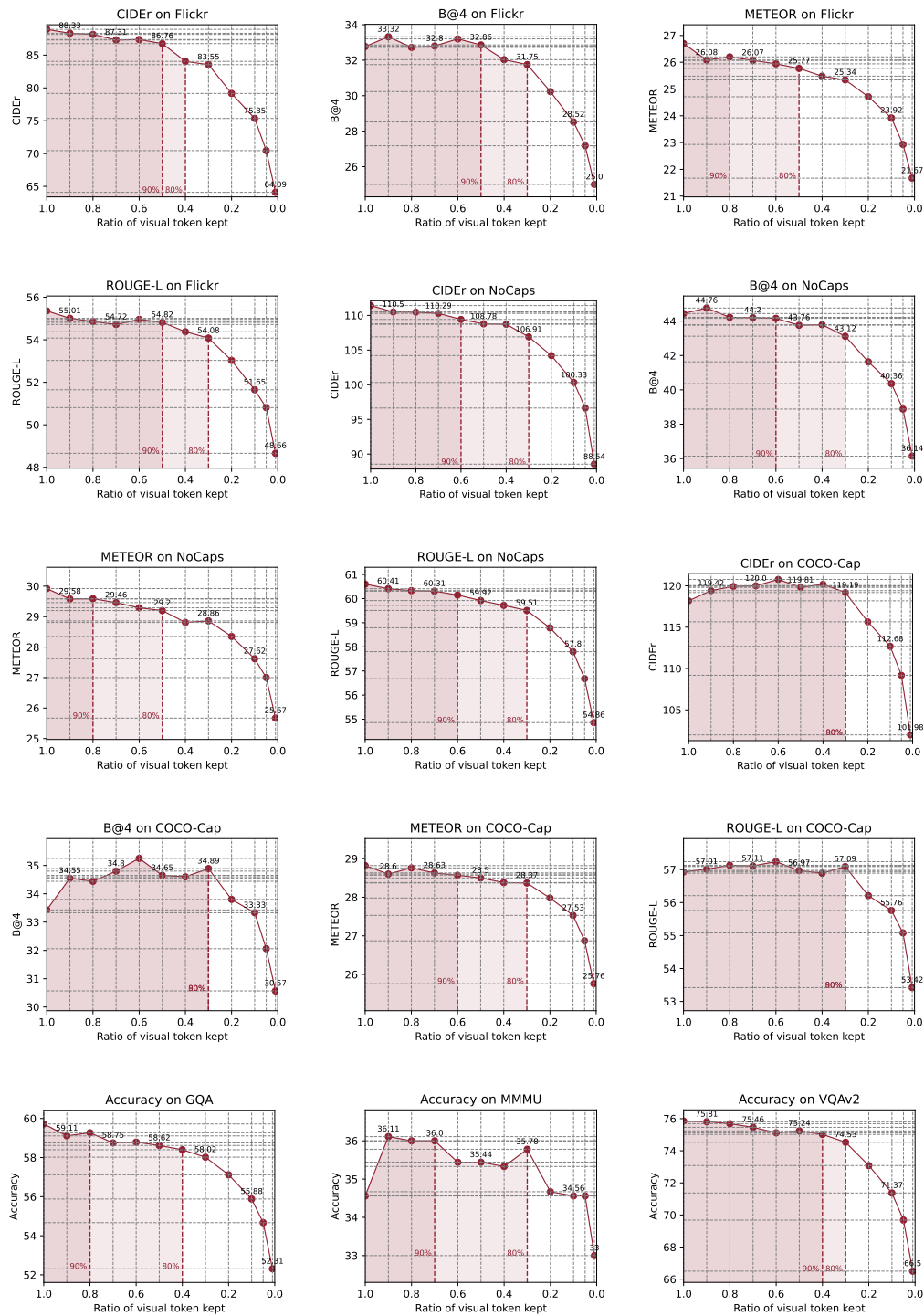


Figure F9: Ablation study of token merging on image captioning on Flickr (Young et al., 2014), NoCaps (Agrawal et al., 2019), COCO-Cap (Lin et al., 2014), visual question answering in GQA (Hudson & Manning, 2019), MMMU (Yue et al., 2023), VQAv2 (Goyal et al., 2017). We found that token merging significantly reduces the number of tokens while maintaining minimal performance drop, and even showing improvement in some tasks. We highlight the token merging ratio when achieving 90% and 80% performance with the dash line and filled area.

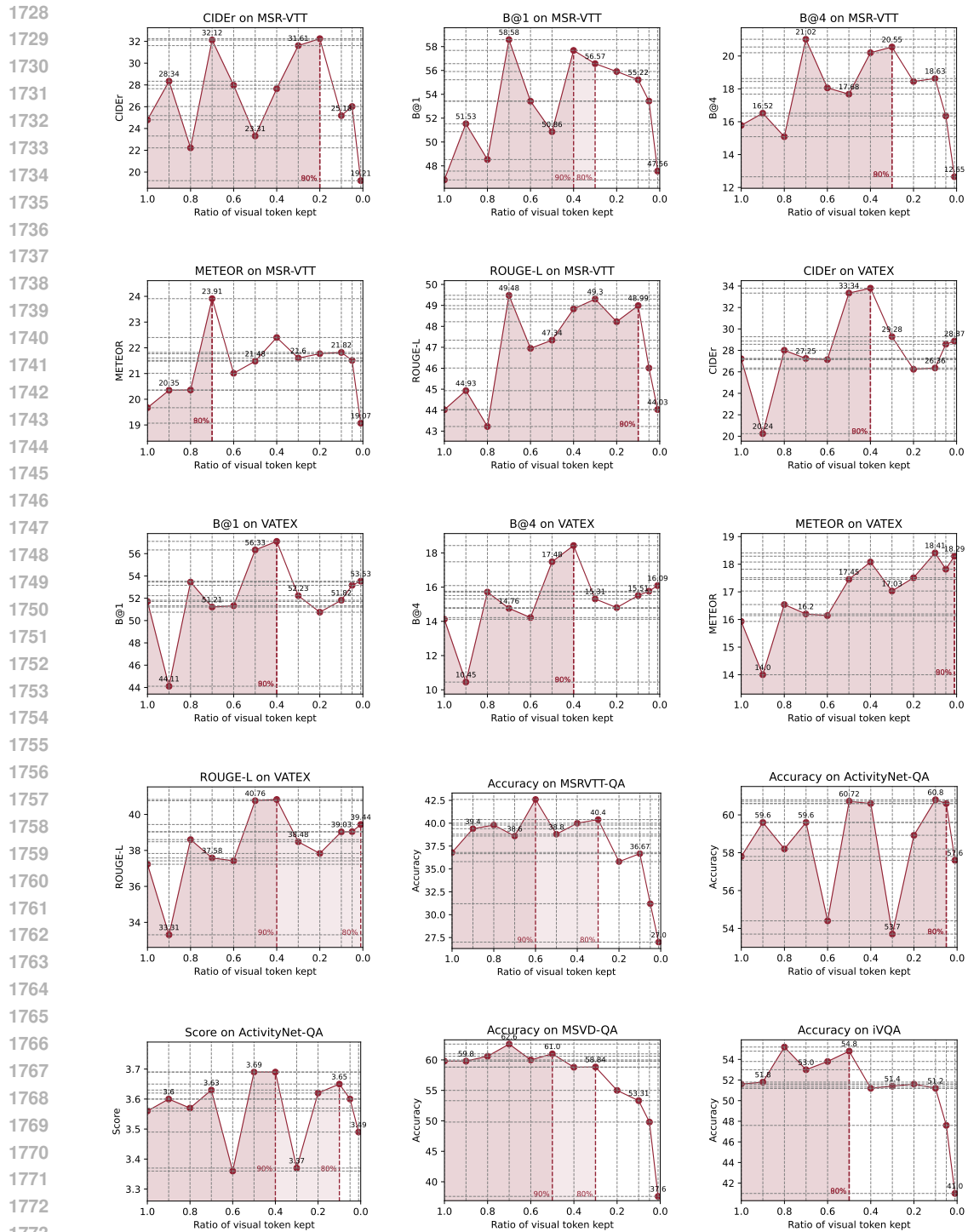


Figure F10: Ablation study of token merging on video captioning on MSRVTT (Xu et al., 2016), VATEX (Wang et al., 2019), video question answering on MSRVTT-QA (Xu et al., 2016), ActivityNet-QA (Yu et al., 2019), MSVD-QA (Xu et al., 2017), iVQA (Liu et al., 2018). We found that token merging significantly reduces the number of tokens while maintaining minimal performance drop, and even showing improvement in some tasks. We highlight the token merging ratio when achieving 90% and 80% performance with the dash line and filled area.

1782
1783
1784
1785
1786
1787
1788
1789
1790
1791
1792
1793
1794
1795
1796
1797
1798
1799
1800
1801
1802
1803
1804
1805
1806
1807
1808
1809
1810
1811
1812
1813
1814
1815
1816
1817
1818
1819
1820
1821
1822
1823
1824
1825
1826
1827
1828
1829
1830
1831
1832
1833
1834
1835

Table G6: Summary of datasets used for training AURORACAP in Pretraining stage.

Task	# Sample	Dataset
Image Captioning	1.3M	LAION-CC-SBU-595K (Liu et al., 2024b), ShareGPT4V (Chen et al., 2023a), ALLaVA-Caption-LAION-4V (Chen et al., 2024a), ALLaVA-Caption-VFLAN-4V (Chen et al., 2024a), DenseFusion (Li et al., 2024e)

Table G7: Summary of datasets used for training AURORACAP in Vision stage. For classification, Reasoning, VQA, and Generation tasks, we adopt the dataset processed by M³IT (Li et al., 2023c) to fit the training objective of language models.

Task	# Sample	Dataset
Captioning	1,925K	ShareGPT4V-PT (Chen et al., 2023a), TextCaps (Sidorov et al., 2020), Image-Paragraph-Captioning (Krause et al., 2017)
Object-centric	438K	COST (Jain et al., 2023), ChatterBox (Tian et al., 2024), V* (Wu & Xie, 2023)
Classification	238K	COCO-GOI (Lin et al., 2014), COCO-Text (Veit et al., 2016), ImageNet (Rusakovsky et al., 2015), COCO-ITM (Lin et al., 2014), e-SNLI-VE (Kayser et al., 2021), Mocheg (Yao et al., 2023), IQA (Duanmu et al., 2021)
Reasoning	100K	CLEVR (Johnson et al., 2017), NLVR (Suhr et al., 2017), VCR (Zellers et al., 2019), VisualMRC (Tanaka et al., 2021), Winoground (Thrush et al., 2022)
VQA	3,518K	VQA v2 (Goyal et al., 2017), Shapes VQA (Andreas et al., 2016), DocVQA (Mathew et al., 2021), OK-VQA (Marino et al., 2019), Text-VQA (Singh et al., 2019), OCR-VQA (Mishra et al., 2019), A-OK-VQA (Schwenk et al., 2022), ScienceQA (Lu et al., 2022), ST-VQA (Biten et al., 2019), ViQuAE (Lerner et al., 2022), LLaVA-OneVision (Li et al., 2024a)
Generation	145K	Visual Storytelling (Huang et al., 2016), Visual Dialog (Das et al., 2017), Multi30k (Elliott et al., 2016)
Chinese	193K	COCO-Caption CN (Li et al., 2019), Flickr-8k-Caption CN (Li et al., 2016), multimodal Chat (Zheng et al., 2021), FM-IQA (Gao et al., 2015), ChineseFoodNet (Chen et al., 2017)
Total	6.6M	For all datasets, we uniformly sample without duplication.

Table G8: Summary of datasets used for training AURORACAP in Language stage.

Task	# Sample	Dataset
Image Captioning	1,779K	ShareGPT4V (Chen et al., 2023a), ALLaVA-Caption-LAION-4V (Chen et al., 2024a), ALLaVA-Caption-VFLAN-4V (Chen et al., 2024a), DenseFusion (Li et al., 2024e), FaceCaption (Dai et al., 2024a)
Video Captioning	1,659K	MiraData (Ju et al., 2024), LLaVA-Hound (Zhang et al., 2024c), ShareGPT4Video (Chen et al., 2024d), Private Data
Image Instruction	9,742K	LLaVA-Mix-665K (Liu et al., 2023), LVIS-Instruct4V (Wang et al., 2023), ALLaVA-Instruct-LAION-4V (Chen et al., 2024a), ALLaVA-Instruct-VFLAN-4V (Chen et al., 2024a), Cambrian (Tong et al., 2024a), M4-Instruct (Liu et al., 2024a)
Video Instruction	268k	LLaVA-Hound (Zhang et al., 2024c), ShareGPT4Video (Chen et al., 2024d)
Language-only	143K	Evol-Instruct-GPT4-Turbo-143K (Chen et al., 2024a)
Total	15.0M	We duplicate video captioning and instruction datasets twice.

1836
 1837
 1838
 1839
 1840
 1841
 1842
 1843
 1844
 1845
 1846
 1847
 1848
 1849
 1850
 1851
 1852
 1853
 1854
 1855
 1856
 1857
 1858
 1859
 1860
 1861
 1862
 1863
 1864
 1865
 1866
 1867
 1868
 1869
 1870
 1871
 1872
 1873
 1874
 1875
 1876
 1877
 1878
 1879
 1880
 1881
 1882
 1883
 1884
 1885
 1886
 1887
 1888
 1889

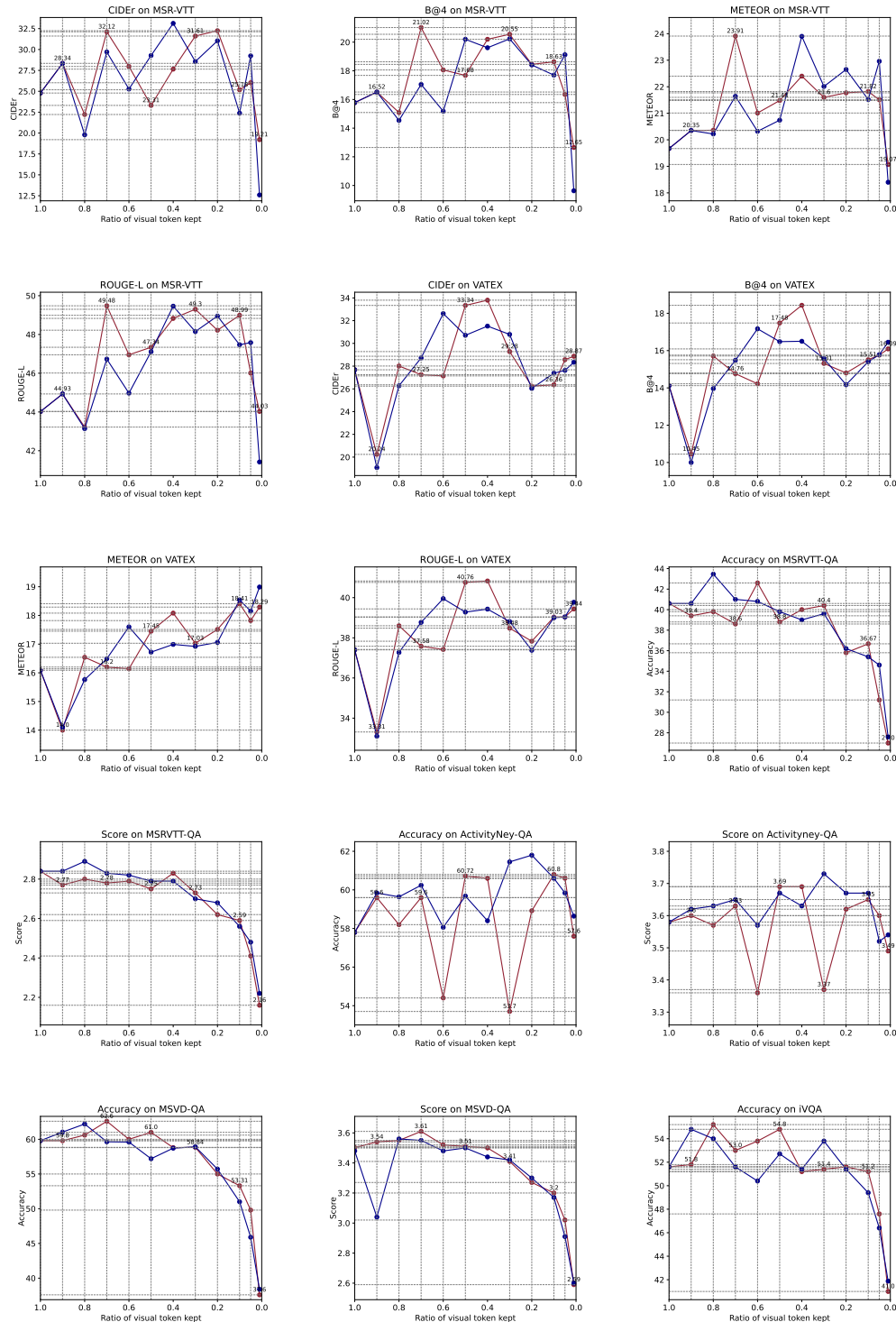


Figure F11: Comparison between performance with and without the inclusion of full first-frame visual tokens during inference on video captioning on MSRVTT (Xu et al., 2016), VATEX (Wang et al., 2019), video question answering on MSRVTT-QA (Xu et al., 2016), ActivityNet-QA (Yu et al., 2019), MSVD-QA (Xu et al., 2017), iVQA (Liu et al., 2018). As the visual token kept ratio varies, the blue curve indicates performance with slowfast inference, while the red curve represents performance without slowfast inference.

1890
 1891
 1892
 1893
 1894
 1895
 1896
 1897
 1898
 1899
 1900
 1901
 1902
 1903
 1904
 1905
 1906
 1907
 1908
 1909
 1910
 1911
 1912
 1913
 1914
 1915
 1916
 1917
 1918
 1919
 1920
 1921
 1922
 1923
 1924
 1925
 1926
 1927
 1928
 1929
 1930
 1931
 1932
 1933
 1934
 1935
 1936
 1937
 1938
 1939
 1940
 1941
 1942
 1943

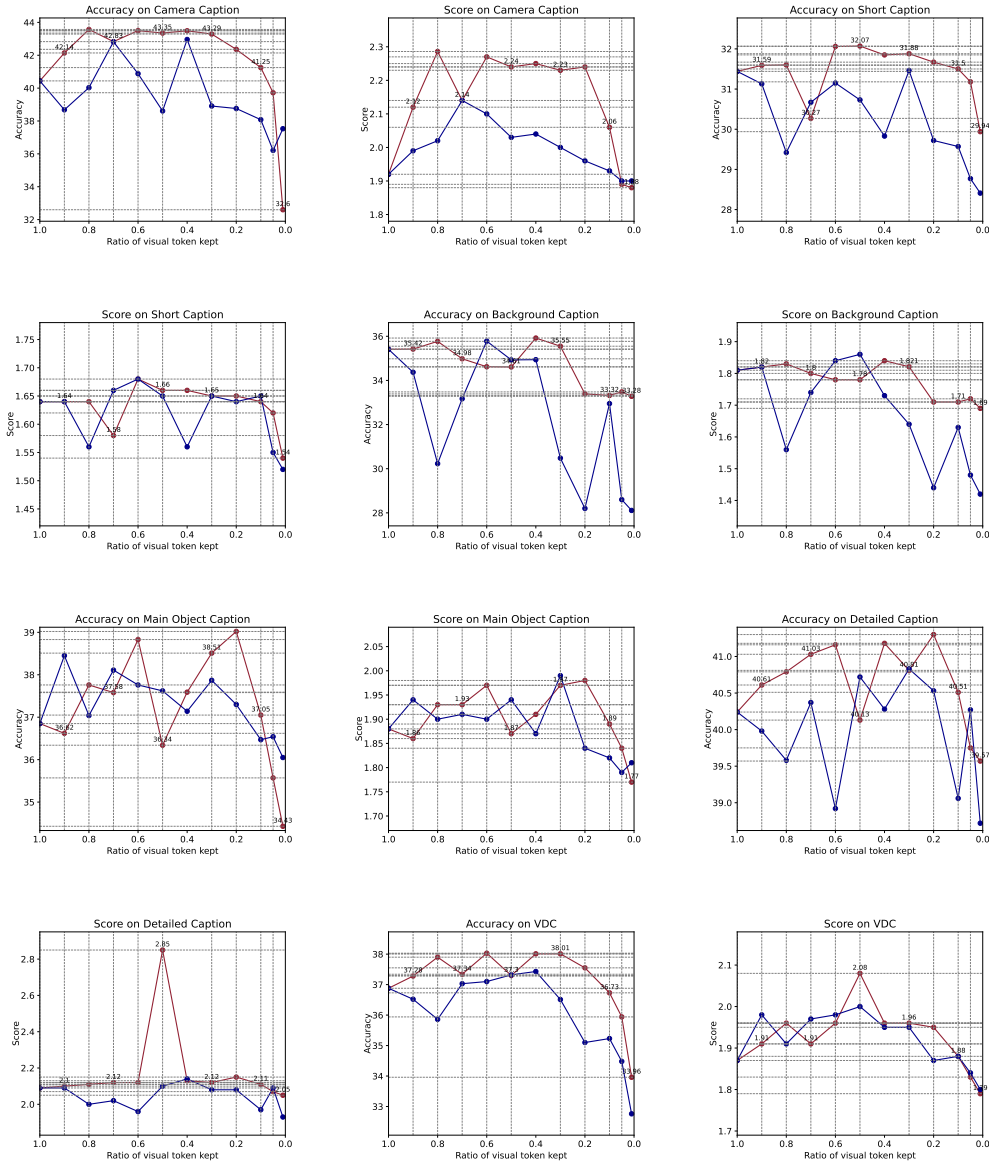


Figure F12: Comparison between performance with and without the inclusion of full first-frame visual tokens during inference on VDC. As the visual token kept ratio varies, the blue curve indicates performance with slowfast inference, while the red curve represents performance without slowfast inference.

1944
1945
1946
1947
1948
1949
1950
1951
1952
1953
1954
1955
1956
1957
1958
1959
1960
1961
1962
1963
1964
1965
1966
1967
1968
1969
1970
1971
1972
1973
1974
1975
1976
1977
1978
1979
1980
1981
1982
1983
1984
1985
1986
1987
1988
1989
1990
1991
1992
1993
1994
1995
1996
1997

Table G9: Training hyper-parameters for AURORACAP.

Hyper-parameters	Pretraining stage	Vision stage	Language stage
trainable parameters	MLP	ViT + MLP	ViT + MLP + LLM
warmup schedule	linear		
warmup start factor	1e-5		
warmup ratio	0.03		
learning rate schedule	cosine decay		
optimizer	AdamW (Loshchilov & Hutter, 2017)		
optimizer hyper-parameters	$\beta_1, \beta_2 = (0.9, 0.999)$		
weight decay	0.1		
max norm	1		
epoch	1		
peak learning rate	2e-4	1e-4	2e-5
total equivalent batch size	512	6,144	768
token keep proportion	100%	100%	10%

Table H10: Evaluation settings summary for each benchmarks. For all benchmarks we set temperature, top p, number of beams to 0, 0, 1 respectively.

Benchmark	# Sample	# Tokens	Prompt
Flickr (Plummer et al., 2015)	31,784	64	Provide a one-sentence caption for the provided image.
NoCaps (Agrawal et al., 2019)	4,500	64	Provide a one-sentence caption for the provided image.
COCO-Cap (Lin et al., 2014)	5,000	64	Provide a one-sentence caption for the provided image.
ChartQA (Masry et al., 2022)	2,500	16	Answer the question with a single word.
DocVQA (Mathew et al., 2021)	5,349	32	Answer the question using a single word or phrase.
TextCaps (Sidorov et al., 2020)	3,166	64	Provide a one-sentence caption for the provided image.
GQA (Hudson & Manning, 2019)	12,578	16	Answer the question using a single word or phrase.
POPE (Li et al., 2023h)	9,000	128	Answer the question using a single word or phrase.
MMMU (Yue et al., 2023)	900	16	Answer with the option letter from the given choices directly. Answer the question using a single word or phrase.
VQA _{v2} (Goyal et al., 2017)	214,354	16	Answer the question using a single word or phrase.
MSR-VTT (Xu et al., 2016)	1,000	64	Provide a one-sentence caption for the provided video.
VATEX (Wang et al., 2019)	4,478	64	Provide a brief single-sentence caption for the last video below.
MSVD-QA (Xu et al., 2017)	1,161	64	Answer the question using a single word or phrase.
ActivityNet-QA (Yu et al., 2019)	8,000	64	Answer the question using a single word or phrase.
MSRVTT-QA (Xu et al., 2017)	6,513	64	Answer the question using a single word or phrase.
iVQA (Yang et al., 2021)	6,000	64	Answer the question using a single word or phrase.

I LIMITATIONS

Table I11: Comparison AURORACAP with LLM-based SoTA methods on visual question answering benchmarks under zero-shot setting.

Model	LLM	MMMU (900) Acc	GQA (12,578) Acc	POPE (9,000) F1	VQAv2 (214,354) Acc
LLaVA-1.5-7B	Vicuna-1.5-7B	35.30	61.97	85.87	76.64
LLaVA-1.5-13B	Vicuna-1.5-13B	34.80	63.24	85.92	78.26
LLaVA-1.6-7B	Vicuna-1.5-7B	35.10	64.23	86.40	80.06
LLaVA-1.6-13B	Vicuna-1.5-13B	35.90	65.36	86.26	80.92
AURORACAP-7B	Vicuna-1.5-7B	36.11	59.72	83.31	75.85

Table I12: Limitation in terms of OCR capability compared with LLaVA models. Appendix H shows the introduction and metrics of each benchmark.

Model	LLM	ChartQA (2,500) Acc	DocVQA (5,349) Acc	TextCaps (3,166) Acc
LLaVA-1.5-7B	Vicuna-1.5-7B	18.24	28.08	98.15
LLaVA-1.5-13B	Vicuna-1.5-13B	18.20	30.29	103.92
LLaVA-1.6-7B	Vicuna-1.5-7B	54.84	74.35	71.79
LLaVA-1.6-13B	Vicuna-1.5-13B	62.20	77.45	67.39
AURORACAP-7B	Vicuna-1.5-7B	25.88	34.60	93.33

We evaluate AURORACAP on various visual question answering benchmarks as shown in Table I11. Since the performance of the VQA task heavily depends on the performance of the LLM, we chose the same LLM for a fair comparison. Also, due to the limitation of OCR-related samples in training dataset, AURORACAP does not perform well in OCR at current stage as shown in Table I12.

J ADDITIONAL EVALUATION METRICS ANALYSIS

In this section, we make the analysis about more evaluation metrics on VDC other than VDCSCORE. As shown in Figure J13, we found that the correlation between CLIP score and human ratings is low (0.39), which may be due to the fact that, in a lengthy caption, there may be only one or two fine-grained errors that the CLIP text encoder lacks the capability to detect. Meanwhile, we test the impact of different numbers of QA pairs on the results when calculating VDCSCORE. As shown in the Figure J13, more QA pairs produced more robust test results. VDCSCORE shows over 0.86 of pearson correlation with human when using 20 QA pairs.

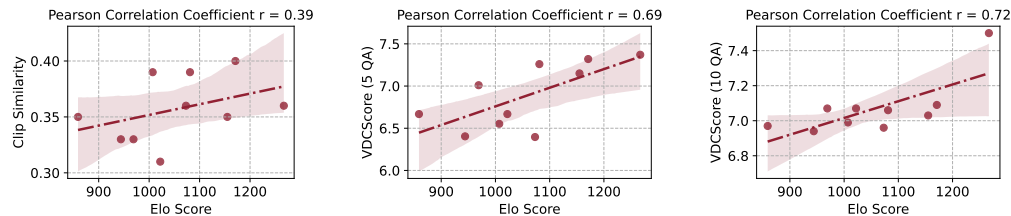


Figure J13: Correlation between the CLIP evaluation scores, different number of QA pairs used in VDCSCORE and human elo ranking on VDC.

K VDC GENERATION PROMPT TEMPLATE

Following (Ju et al., 2024), we utilize LLM to generate structured detailed captions. Given an input video, LLM return five detailed captions, including camera caption, short caption, background caption, main object caption and detailed caption for the entire video guided by our designed prompt template. The complete prompt is shown as followings:

Type Prompt

SYSTEM You are describing the video. Please provide detailed captions of the video from different aspects.

User Please provide detailed and comprehensive captions for the following content: 1. Short Caption: Summarize the video in one detailed sentence, capturing key actions and the overall mood. 2. Background Caption: Provide a detailed description of the background, including objects, location, weather, time, and any dynamic elements such as movements in the environment. 3. Main Object Caption: Give a thorough description of the main subject’s actions, attributes, interactions, and movements throughout the video frames, including changes in posture, expression, or speed. 4. Camera Caption: Describe the camera work in detail, including shot types, angles, movements, transitions, and any special effects used to enhance the video. 5. Reference Caption: Generate a detailed dense caption for the video that is at least 300 words long. The caption should capture all visible actions, environmental details, and the overall emotional atmosphere in depth. Describe in detail the interactions between the main subjects and their environment, including subtle nuances of their movements or expressions. Elaborate on the sounds, textures, and other sensory experiences depicted in the video. Discuss the camera techniques used extensively, including shot types, angles, movements, and transitions. Highlight the mood and tone of the video throughout, creating a rich narrative that connects viewers emotionally to the scene. Include comprehensive descriptions of background elements that add context and depth, such as weather conditions, time of day, and cultural or historical settings. Make sure to provide a vivid portrayal that is engaging, informative, and rich enough for AI to re-generate the video content.

No need to provide summary content. Do not describe each frame individually. Avoid using phrases like ‘first frame’. The description should be rich enough for AI to re-generate the video. Please generate the response as a Python dictionary string with keys like ‘short caption’. DO NOT PROVIDE ANY OTHER OUTPUT TEXT OR EXPLANATION. Only provide the Python dictionary string.

These are the frames from the video: [VIDEO KEYFRAME INPUT]

GPT-4o Short Caption: In a sunny outdoor setting, two workers engage in a collaborative effort to prepare a gravel base for a construction project, showcasing teamwork and focus.

Camera Caption: The camera captures the scene from a low angle, providing a unique perspective that emphasizes the workers’ actions and the surrounding environment. The shots are primarily medium close-ups, focusing on the workers’ upper bodies and hands as they interact. The camera occasionally shifts to a wider angle, revealing more of the workspace and background elements. There are smooth transitions between shots, maintaining a steady flow that enhances the viewer’s engagement with the unfolding narrative. The use of a slightly fish-eye lens effect adds depth to the scene, making the environment feel more immersive.

Background Caption: The scene is set in a residential area with a well-maintained lawn and a brick wall partially constructed in the background. The ground is covered with a white plastic sheet, and scattered gravel is visible. A few wooden planks lie on the ground, and tools are scattered around, including a black water bottle and a power tool.

Main Object Caption: The main subjects are two workers, one wearing a gray sweatshirt and gloves, and the other dressed in casual work attire. They are actively engaged in conversation, with the first worker gesturing with his hands to emphasize points while explaining the task at hand. His posture is relaxed yet focused, indicating a collaborative atmosphere. The second worker listens attentively, occasionally nodding and responding with gestures, showcasing a dynamic interaction. Both workers exhibit a sense of camaraderie and professionalism as they prepare for the next steps in their project.

Reference Caption: The video unfolds ... (300 words) ... through them.

User The video has been describe from the following aspects:1. short caption: short caption, 2. background caption: background caption, 3. main object caption: main object caption, 4. camera caption: camera caption, 5.Reference Caption: reference caption Please generate a detailed dense caption for the video that is pretty long. You should expand the reference caption upon the information provided in the short caption, background caption, main object caption, and camera caption. Ensure that the detailed caption does not introduce any new entities or relationships that were not mentioned in the previous captions. Make sure to provide a vivid portrayal that is engaging, informative, and rich enough for AI to re-generate the video content. "Avoid using phrases like ‘first frame’, ‘short caption’, ‘background caption’, ‘main object caption’, and ‘camera caption’. The description should be rich enough for AI to re-generate the video.

GPT-4o Detailed Caption: The video opens with ... (500 words) ... literature that surrounds them.

User [Manually check and refine]

L QUESTION-ANSWER PAIRS GENERATION PROMPT TEMPLATE OF VDCSCORE

To decompose the ground-truth structured detailed captions in VDC, we utilize GPT-4o as the LLM assistant to generate numerous short question-answer pairs for subsequent evaluation. The full prompt and example cases are presented as followings:

Type Prompt

SYSTEM You are an intelligent chatbot designed for generating 20 question-answer pairs given a detailed description of a video or image. You are describing the video.

Here's how you can accomplish the task: **INSTRUCTIONS:** - Cover the main objects and actions in the video or image.

- The questions should be open-ended and start with 'What', 'Who', 'Where', 'When', 'Why', 'How', etc.

- The answer should be a short sentence or phrase.

- Generate 20 question-answer pairs.

User Please generate 20 question-answer pairs given a detailed description of a video or image: detailed description: The camera work is dynamic, featuring a mix of close-up shots and wider angles that provide context to the environment. The shots are slightly shaky, adding a sense of realism and immersion to the viewer. Transitions between shots are smooth, with the camera often panning or tilting to follow the subject's movements. The use of low light creates a moody atmosphere, with shadows enhancing the visual interest of the scene . . .

Please generate the response in the form of a Python list of tuple with the question and the corresponding answer. **DO NOT PROVIDE ANY OTHER OUTPUT TEXT OR EXPLANATION.** Only provide the Python list of tuple. For example, your response should look like this: [(the question 1, the answer 1), (the question 2, the answer 2), . . .].

GPT-4o [{"question": "What is the style of camera work in the video?", "answer": "dynamic", "question": "What is the effect of shaky shots in the video?", "answer": "realism and immersion", "question": "What type of transitions are used in the video?", "answer": "smooth", "question": "Why is the moody atmosphere created in the video?", "answer": "through low light", "question": "What type of camera movement is achieved through panning and tilting?", "answer": "following the subject's movements", "question": "What is the effect of the camera movement on the viewer?", "answer": "sense of realism and immersion", . . .}]

User [Manually check and refine]

M MORE STATISTICS INFORMATION OF VDC

Figure M14 indicates the word distribution of the structured captions in VDC. Table M13 illustrates the distribution of the question categories we provided for VDCSCORE calculation.



Figure M14: Word cloud of different structured captions in VDC, showing the diversity.

Table M13: Distribution of the question categories in VDCSCORE.

Type	Background	Camera	Short	Main object	Detailed
Environment & Scene	3,464	2,543	4,401	3,097	3,549
Character & Object	6,272	3,779	4,834	6,035	6,440
Intent & Outcomes	4,585	5,105	5,067	4,474	4,640
Action	2,861	1,198	1,857	3,192	1,932
Attributes & Relationship	944	334	1,388	1,478	1,280

N MORE STATISTICS INFORMATION OF VDCSCORE

We generate a total of 96,902 question-answer pairs for VDC, with an average of 18.87 pairs per detailed caption. As depicted in Figure N15, each section of the structured captions includes a similar number of question-answer pairs. Additionally, Figure N16 presents the distribution of question types generated for VDC. To enhance the evaluation of detailed captions, we configure all questions as open-ended. Environment & Scene encompasses inquiries about location, environment, atmosphere, scene, and time. Character & Object focuses on entities within the caption, such as people, animals, plants, and objects, while Attribute & Relation examines their attributes and interrelations. Intent & Outcomes addresses deeper interpretative questions regarding methods, purposes, reasons, and outcomes. We further analyze the distribution of generated question types within structured captions. Main object captions predominantly feature Character & Object questions, whereas Environment & Scene questions are more prominent in background captions, and Camera questions constitute a larger proportion in camera.

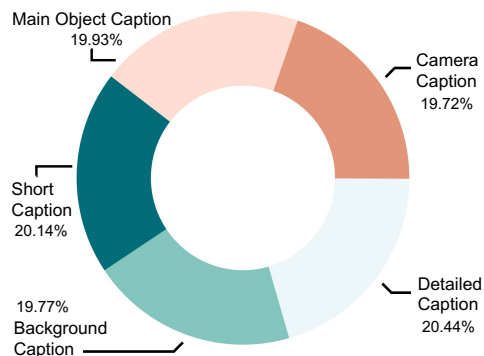


Figure N15: Question-answer pairs proportion in structured captions.

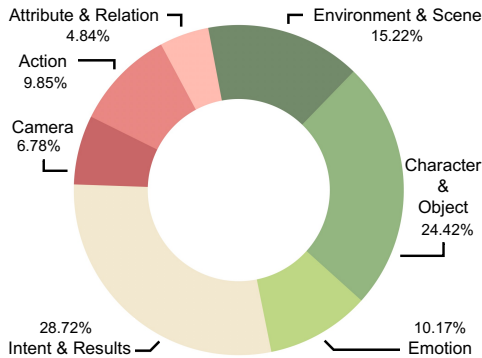


Figure N16: Distribution of question type in VDCSCORE.

O CALCULATION OF ELO RANKING

In this section, we present the methodology for evaluating and ranking AURORACAP and various models using the Elo rating system as shown in Figure O17. The parameters used in the simulation are summarized in Table O14.

1. For all models participating in the ELO ranking, we collect the output captions for each video.
2. As shown in Figure O17, we develop a frontend tool to randomly select captions generated by two different models for the same video. Without revealing the model IDs, human evaluators then chose the caption they found better.
3. We record comparison results and calculated the ELO values based on the parameters in Table O14.
4. In Figure 5, we calculate the Pearson correlation between different metrics and human ELO values, ultimately showing that our proposed VDC metric is the closest to human evaluations.

2214
2215
2216
2217
2218
2219
2220
2221
2222
2223
2224
2225
2226
2227
2228
2229
2230
2231
2232
2233
2234
2235
2236
2237
2238
2239
2240
2241
2242
2243
2244
2245
2246
2247
2248
2249
2250
2251
2252
2253
2254
2255
2256
2257
2258
2259
2260
2261
2262
2263
2264
2265
2266
2267

Table O14: Elo parameter setting.

Parameter	Number
initial Elo mean	1,000
Elo standard deviation	300
base of logarithm	10
scaling factor	400
K-factor	32
minimum Elo rating	700
number of simulated matches	2,778

Caption Comparison Interface

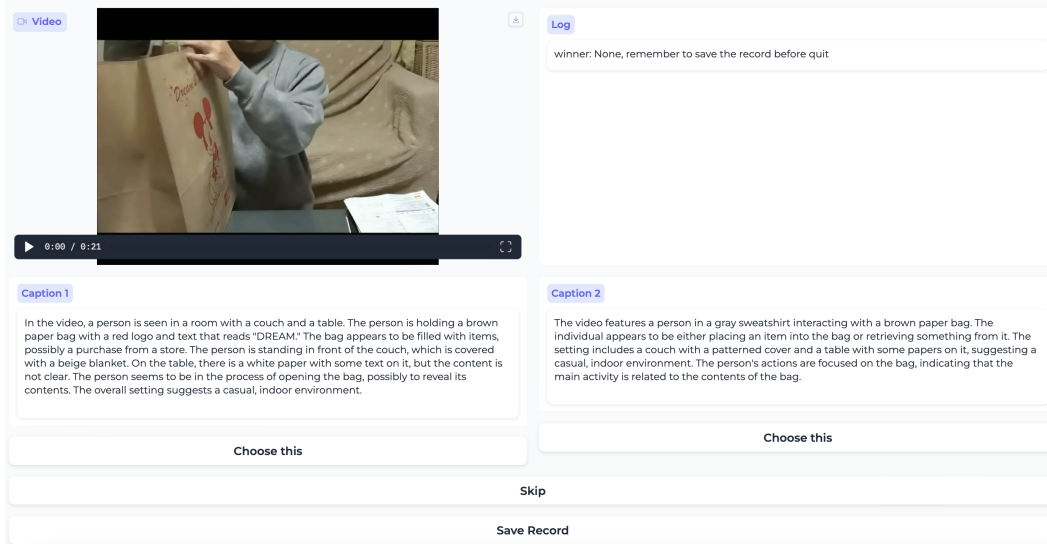


Figure O17: GUI screen for Elo ranking.

P CASE STUDY

We perform an extensive case study of AURORACAP on a variety of videos for video detailed captioning. As shown as followings, AURORACAP is capable of providing excellent detailed captions regarding the camera motion, background and main object with less hallucination.



Figure P18: Video example of MSR-VTT (Xu et al., 2016) benchmark.

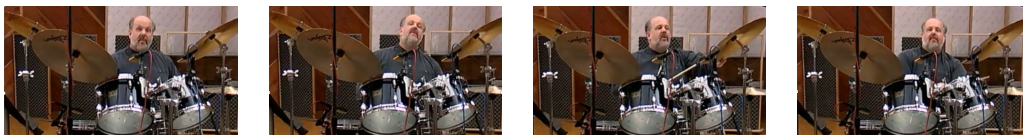
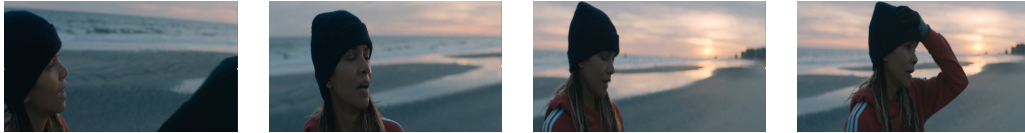


Figure P19: Video example of VATEX (Wang et al., 2019) benchmark.

2268



2269

2270

2271

2272

2273

Figure P20: Video example.

2274

2275

2276



2277

2278

2279

2280

2281

Figure P21: Video example.

2282

2283

2284



2285

2286

2287

2288

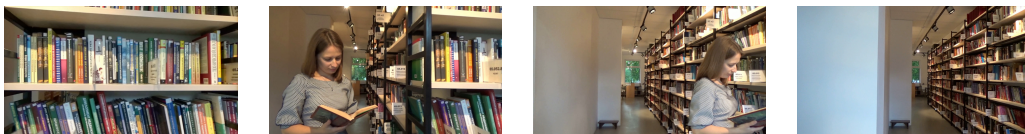
2289

Figure P22: Video example.

2290

2291

2292



2293

2294

2295

2296

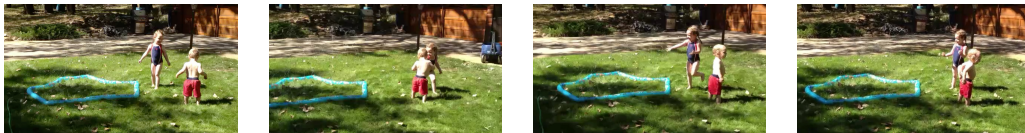
2297

Figure P23: Video example.

2298

2299

2300



2301

2302

2303

2304

2305

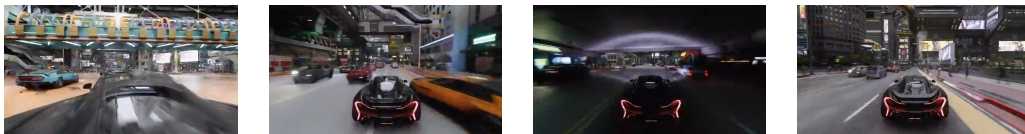
Figure P24: Video example.

2306

2307

2308

2309



2310

2311

2312

2313

2314

Figure P25: Video example.

2315

2316

2317

Example Caption

2318

Figure P18 [short caption] A man with a mustache and a woman with a ponytail are sitting at a table.

2319

Figure P19 [short caption] A man plays the drums in a recording studio.

2320

Figure P20 [detailed caption] The video depicts a serene beach scene where a young woman stands on the sandy shore, gazing out towards the ocean. She is wearing a black beanie and a pink jacket, adding a pop of color to the otherwise muted scene. The beach, a vast expanse of sand, stretches out

2321

2322 in front of her, meeting the ocean at the horizon. The ocean, a vast body of water, is visible
 2323 in the background. The beach is bathed in a soft, diffused light, creating a dreamy atmosphere.
 2324 The girl’s gaze is directed towards the horizon, suggesting a sense of wonder or contemplation.
 2325 The image is slightly blurred, adding a dreamy quality to the scene. The woman’s position on
 2326 the beach, coupled with the gentle waves of the ocean, suggests a moment of contemplation or
 2327 admiration. The relative positions of the objects suggest a peaceful day at the beach, with the girl
 2328 possibly enjoying the serene view of the ocean. The colors are mostly muted, with the girl’s pink
 2329 jacket standing out against the sandy beach and the blue ocean. The blurred background and the
 2330 out-of-focus elements, such as the ocean and the sky, contribute to the sense of tranquility and
 2331 focus on the woman. There is no text present in the video, and the colors are muted, with the
 2332 exception of the pink jacket, which stands out against the more subdued tones of the surroundings.

2332 Figure P21 [detailed caption] The video features a man with a beard and long hair, lying on the ground with
 2333 his head resting on a tree trunk. He is wearing a colorful shirt with a mix of orange and green
 2334 patterns. The man’s face is partially obscured by the tree trunk, but his eyes are visible, looking
 2335 upwards. He appears to be smiling or laughing, with his mouth open. The man’s arms are crossed
 2336 over his chest, suggesting a relaxed or playful posture. The background is blurred, but it appears
 2337 to be a natural outdoor setting, possibly a forest or park. In the background, another person is
 2338 partially visible, their presence subtly hinted at by a hand reaching out from the left side of the
 2339 frame. The colors in the video are warm, with the man’s shirt standing out against the muted
 2340 background. The man’s hair and beard are dark, and he has a light complexion. The overall mood
 2341 of the video is lighthearted and carefree. There are no visible texts or other objects in the video,
 2342 and the relative positions of the objects remain constant with the man in the foreground and the
 2343 second person in the background.

2342 Figure P22 [background caption] The background features a race track with visible tire marks and barriers,
 2343 surrounded by grassy areas and a few scattered trees. The track is set in a rural or semi-rural
 2344 location, with hills in the distance and a cloudy sky overhead, suggesting overcast weather
 2345 conditions. The track itself appears well-maintained with a smooth surface, designed for high-
 2346 speed racing. The weather, indicated by the cloudy sky, contributes to the overall ambiance of the
 2347 scene, enhancing the sense of a cool, possibly early morning or late afternoon setting.

2347 Figure P23 [camera caption] The camera maintains a steady, frontal view throughout the video, capturing the
 2348 woman’s expressions and the intricate details of the bookshelves. The camera starts at the right
 2349 edge of the bookshelf, moving across the shelf, and ends at the left edge of the bookshelf. The
 2350 framing is consistent, focusing on the woman and the bookshelves, with the camera positioned at a
 2351 medium distance to the subject. This movement provides a comprehensive view of the bookshelf,
 2352 showcasing the variety of books and their arrangement on the shelves. The camera occasionally
 2353 pans to reveal the depth of the library, showcasing the rows of books and the inviting atmosphere.
 2354 The use of natural light enhances the visual appeal, creating a warm and inviting tone throughout
 2355 the video.

2355 Figure P24 [camera caption] The view shot remains relatively static, focusing on the children playing in the
 2356 backyard. The camera angle is at eye level, capturing the scene from a distance that allows both
 2357 children to be visible. There is minimal camera movement, maintaining a steady focus on the
 2358 children and their activities. The sequence of video frames suggests a continuous moment of play
 2359 without significant changes in shooting angles or camera movement.

2359 Figure P25 [main object caption] The main subject in the video, a black car, is seen driving down a street that
 2360 appears to be in a state of disarray. The car moves steadily forward, navigating around obstacles
 2361 such as a blue car parked on the side of the road. The car’s movement is smooth and continuous,
 2362 suggesting it is either in motion or has just come to a stop. The environment around the car is
 2363 chaotic, with debris scattered across the road and signs of destruction, indicating a recent event or
 2364 disaster. The car’s position remains central in the frame, with the camera angle focused on it from
 2365 a slightly elevated perspective, possibly from a vehicle or a structure above.

2366 Q PREDICTED ANSWER EXTRACTION PROMPT TEMPLATE

2367
 2368
 2369 Given the question-answer pairs based on the ground truth caption, we utilize GPT-4o to extract
 2370 predicted answers based on the generated caption by our designed prompt template. The complete
 2371 prompt is shown as followings:

2372 Type Prompt

2373 SYSTEM You are an intelligent chatbot designed for providing accurate answers to questions related to the
 2374 content based on a detailed description of a video or image.
 2375 Here’s how you can accomplish the task:”

2376 **##INSTRUCTIONS:**
 2377 - Read the detailed description carefully.
 2378 - Answer the question only based on the detailed description.
 2379 - The answer should be a short sentence or phrase.

2380 User Please provide accurate answers to questions related to the content based on a detailed description of a
 2381 video or image:
 2382 detailed description: The setting is an urban street with a distinctive red and white painted bike lane,
 2383 which is part of a larger roadway. The lane is marked with white lines and the word "WALK" is
 2384 painted in large, bold letters, indicating a pedestrian crossing area. The pavement is a mix of red brick
 2385 and grey tiles, with a curb separating the bike lane from the adjacent road. The weather appears to be
 2386 clear and sunny, casting sharp shadows on the ground, suggesting it is daytime. There are no other
 2387 vehicles or pedestrians in sight, and the road is empty, which could imply a quiet time of day or a less
 2388 busy area. The presence of a yellow circular object on the handlebar of the bicycle is notable, possibly
 2389 a bell or a light.
 2390 question: What objects are the cyclist's hands interacting with?
 2391 **DO NOT PROVIDE ANY OTHER OUTPUT TEXT OR EXPLANATION.** Only provide short but
 2392 accurate answer.

2391 GPT-4o The cyclist's hands are interacting with the bicycle handlebars.

2393 **R CORRECTNESS EVALUATION PROMPT TEMPLATE**

2395 Following (Maaz et al., 2023), we evaluate the correctness and score of the predicted answers with the
 2396 assistant of GPT-4o. Given the question, correct answer, and predicted answer from the generated
 2397 caption, GPT-4o should return the *True* or *False* judgement and relative score (0 to 5). The complete
 2398 prompt is shown as followings:

2399 **Type Prompt**

2400 SYSTEM You are an intelligent chatbot designed for evaluating the correctness of generative outputs for question-
 2401 answer pairs.
 2402 Your task is to compare the predicted answer with the correct answer and determine if they match
 2403 meaningfully. Here's how you can accomplish the task:

2404 **##INSTRUCTIONS:**

- 2405 - Focus on the meaningful match between the predicted answer and the correct answer.
- 2406 - Consider synonyms or paraphrases as valid matches.
- 2407 - Evaluate the correctness of the prediction compared to the answer.

2408 User Please evaluate the following video-based question-answer pair:

2409 Question: What type of surface can be seen covering the floor?

2410 Correct Answer: carpet

2411 Predicted Answer: Carpeted surface.

2412 Provide your evaluation only as a yes/no and score where the score is an integer value between 0 and
 2413 5, with 5 indicating the highest meaningful match.

2414 Please generate the response in the form of a Python dictionary string with keys 'pred' and 'score',
 2415 where value of 'pred' is a string of 'yes' or 'no' and value of 'score' is in INTEGER, not STRING.

2416 **DO NOT PROVIDE ANY OTHER OUTPUT TEXT OR EXPLANATION.** Only provide the Python
 2417 dictionary string.

2418 For example, your response should look like this: {'pred': 'yes', 'score': 4.8}.

2419 GPT-4o {'pred': 'yes', 'score': 5}

2420
2421
2422
2423
2424
2425
2426
2427
2428
2429